A mechanism for the elimination of IgE plasma cells

Adam K. Wade-Vallance[1,2,3], Zhiyong Yang[2,3,6], Jeremy B. Libang[2,3], Marcus J. Robinson[2,3,5], David M. Tarlinton[5], and Christopher D. C. Allen[2,3,4*]

[1]Biomedical Sciences Graduate Program, [2]Cardiovascular Research Institute, [3]Sandler Asthma Basic Research Center, and [4]Department of Anatomy, University of California, San Francisco, CA 94143, USA

[5]Department of Immunology & Pathology, Monash University, Melbourne, VIC 3004 Australia

[6]Present address: Department of Immunology Discovery, Genentech, Inc., South San Francisco, CA 94080, USA

*Correspondence should be addressed to:

Christopher D. C. Allen, Ph.D.

Address: UCSF
CVRI, Box 3122
555 Mission Bay Blvd S
San Francisco, CA 94143

Email: Chris.Allen@ucsf.edu

Phone: 415-476-5178

ABSTRACT

The proper regulation of IgE production safeguards against allergic disease, highlighting the importance of mechanisms that restrict IgE plasma cell (PC) survival. IgE PCs have unusually high surface B cell receptor (BCR) expression, yet the functional consequences of ligating this receptor are unknown. Here, we found that exposure of IgE PCs to cognate antigen resulted in BCR signaling that culminated in apoptosis. BCR ligation-induced elimination of IgE plasma cells correlated with the affinity, avidity, amount, and duration of antigen exposure and required the BCR signalosome components Syk, BLNK, and PLCγ2. In mice with a PC-specific impairment of BCR signaling, the abundance of IgE PCs was selectively increased. Conversely, after IgE BCR ligation with a monoclonal antibody, IgE PCs were depleted *in vitro* and *in vivo*. These findings establish that BCR ligation is a mechanism to induce the elimination of IgE PCs, which has important implications for allergen tolerance and immunotherapy as well as anti-IgE monoclonal antibody treatments.

INTRODUCTION

The production of IgE specific for environmental antigens is a critical driver of allergic disease. Normally, the production of IgE is tightly controlled and the abundance of IgE in serum is orders of magnitude less than that of IgG. In the past decade, technical advancements in the detection of rare IgE-expressing cells have rapidly expanded our knowledge of the mechanisms that limit IgE production.

IgE-expressing (IgE) B cell responses are constrained by multiple key regulatory mechanisms. The initial class-switch recombination to IgE requires adequate IL-4 and is profoundly inhibited by IL-21, leading to the generation of limited numbers of IgE B cells (Burgis and Gessner, 2007; Muller et al., 2008; Robinson et al., 2017; Yang et al., 2020). Once generated, IgE B cells exhibit a propensity to undergo rapid differentiation into IgE antibody-secreting cells (plasmablasts or plasma cells [PCs], which we collectively refer to hereafter as PCs for simplicity) (Erazo et al., 2007; Yang et al., 2012). IgE B cells are rare within germinal centers (GCs) and their relative abundance there further diminishes over time (He et al., 2013; Yang et al., 2012). In GCs, B cells undergo iterative cycles of Ig mutation and selection, resulting in antibody refinement and affinity maturation, and ultimately differentiate into long-lived PCs or memory B cells. In contrast, most IgE PCs are short-lived and are generated independently from GCs, while IgE memory B cells have not been reliably detected (Allen, 2022; He et al., 2013; Jimenez-Saiz et al., 2019; Yang et al., 2012).

The skewed cell fate trajectories of IgE B cells are driven by antigen-independent signaling of the IgE B cell receptor (BCR). When B cells were cultured in the absence of cognate antigen, the expression of membrane IgE (mIgE) resulted in enhanced PC differentiation compared with the expression of other BCR isotypes (Haniuda et al., 2016; Yang et al., 2016). In addition, genetic deficiency or pharmacological inhibition of proteins involved in BCR signal transduction, such as Syk, Btk, BLNK, and CD19, resulted in a decrease in the frequency of IgE PCs in cell culture without antigen (Haniuda et al., 2016; Yang et al., 2016). A recent CRISPR screen in cell culture (Newman and Tolar, 2021) further highlighted the contribution of BCR signaling components to IgE PC differentiation without antigen. Overall, these data are consistent with a model that the IgE BCR has antigen-independent activity that promotes PC differentiation (Haniuda et al., 2016; Yang et al., 2016).

Based on this model, we predicted that mice with impaired BCR signal transduction would have reduced IgE PC differentiation, which would result in the enhanced differentiation and/or maintenance of IgE GC B cells. While these mice indeed had increased frequencies of IgE B cells in GCs, unexpectedly they also had increased numbers of IgE PCs (Haniuda et al., 2016; Yang et al., 2016). Moreover, a recent mutagenesis screen in mice found that IgE production was increased when BCR signaling was impaired (SoRelle et al., 2021). One possibility is that the increases in IgE PCs in the context of *in vivo* BCR signaling impairments were due to the enhanced IgE GC B cell responses. Indeed, in BLNK-deficient mice, a sustained increase in the abundance of IgE PCs was observed, and Ig sequencing four weeks after immunization showed somatic mutations consistent with a GC origin (Haniuda et al., 2016). However, we also observed an increase in IgE PCs early after immunization of mice with BLNK-deficiency or with heterozygous mutations in *Syk* (Yang et al., 2016), suggesting these PCs may be generated through the extrafollicular pathway, independently from GCs. We confirmed that most IgE PCs expressed unmutated, germline Ig sequences, consistent with a GC-independent origin, 9 days after immunization of mice with *Syk*-heterozygous activated B cells (Yang et al., 2016). The mechanism by which impairments of BCR signal transduction led to increases in both GC-dependent and GC-independent IgE PC responses *in vivo* remains unclear.

One possibility to account for these findings is that BCR signaling has direct effects on differentiated IgE PCs rather than only their IgE B cell precursors. While the differentiation of B cells into PCs is often thought to coincide with a shift from the expression of membrane Ig (mIg) to secreted Ig (sIg), we and others previously reported that IgE PCs upregulated mIg expression compared with IgE B cells (He et al., 2013; Ramadani et al., 2017; Yang et al., 2012). High mIg expression has also been observed on IgM and IgA PCs, and these BCRs were signaling-competent (Blanc et al., 2016; Pinto et al., 2013). Whether the BCR on IgE PCs is functional has not been directly examined. In addition, while previous studies focused on antigen-independent signaling of the IgE BCR (Haniuda et al., 2016; Yang et al., 2016), antigen stimulation of the BCR would be relevant to real-world immunizations, allergen exposures, allergen immunotherapies, and parasitic worm infections.

Here, we report that high surface mIg expression on IgE PCs corresponds with elevated phosphorylation of Syk, BLNK, and PLCγ2 after stimulation with antigen. Cell culture studies revealed that this BCR signaling depleted antigen-specific IgE PCs in a manner that

corresponded to the strength and duration of BCR stimulation. Consistent with the induction of apoptosis in IgE PCs after cognate antigen exposure, BCR ligation led to caspase-3 activation in IgE PCs, followed by cell death, which was rescued by *Bcl2* overexpression. Antigen-induced IgE PC elimination was also blocked by inhibition of Syk or genetic deficiency in *Blnk* or *Plcg2*, highlighting the importance of the BCR signalosome to this process. *In vivo*, heterozygosity for *Syk* specifically in PCs resulted in an increase in the absolute number and relative frequency of IgE PCs. Conversely, targeting mIgE on IgE PCs with a monoclonal antibody led to the robust depletion of IgE PCs. Based on these findings, we propose that IgE PCs are intrinsically regulated by BCR signaling-induced apoptosis.

RESULTS

IgE PCs have heightened BCR expression and signaling

An unusual feature of IgE responses is that IgE PCs have higher expression of both mIg and sIg than IgE GC B cells (He et al., 2013). However, the relative surface abundance of mIg on IgE PCs compared with cells expressing other BCR isotypes has not been reported. We therefore directly compared the surface BCR expression on IgE PCs to GC B cells and PCs of various isotypes *in vivo*. To control for possible effects of the Ig variable region on surface BCR expression, we utilized B cells from B1-8i (hereafter referred to as B1-8) mice (Sonoda et al., 1997). These B cells express a knock-in heavy chain VDJ specific for the hapten 4-hydroxy-3-nitrophenyl (NP) when paired with Igλ light chains. To compare mIg expression *in vivo*, we adoptively transferred naïve Igλ-enriched B1-8 B cells into *Cd19*$^{-/-}$ recipients, immunized with NP conjugated to chicken gamma globulin (NP-CGG) in alum adjuvant, and then analyzed the surface BCR expression on responding B1-8 cells in the draining lymph nodes (dLNs) by flow cytometry. For equivalent comparison of surface mIg expression, we stained the Ig light chain (LC) on cells with an antibody to Igλ. We observed that IgE PCs had the highest surface mIg expression among all GC B cells and PCs examined, which was more than an order of magnitude higher than IgG1 PCs and IgE GC B cells and was slightly higher (1.5-fold) than IgM PCs (Figure 1A).

We next tested whether ligation of mIg on IgE PCs would trigger an intracellular BCR signaling cascade as has been reported for IgM and IgA PCs (Blanc et al., 2016; Pinto et al., 2013). We injected antigen *in vivo* and examined the activation of intracellular signaling proteins by phosflow 30 minutes later. IgE and IgM PCs exhibited robust phosphorylation of BLNK and PLCγ2, whereas IgG1 PCs did not (Figure 1B), indicating that IgE and IgM PCs can sense and respond to antigen *in vivo*.

To further explore BCR signaling in IgE PCs, we turned to an *in vitro* cell culture system. B cells were cultured with anti-CD40 and IL-4 to induce class-switch recombination and PC differentiation. For studies of BCR expression, we cultured Igλ-enriched B1-8 cells and detected surface BCR expression by flow cytometry with an antibody to the Igλ LC. We found that IgE and IgM PCs had similar BCR expression, which was higher than IgG1 PCs (Figure 1C). These trends were similar to our *ex vivo* observations (Figure 1A), although a further upregulation of surface BCR expression was noted on IgE PCs generated *in vivo* compared with in cell culture.

Surface BCR expression on IgE PCs was also higher than on IgE B cells in cell culture, which had several-fold lower surface BCR expression than IgG1 and IgM B cells. To assess BCR signaling *in vitro*, we cultured polyclonal purified B cells, the vast majority of which express Igκ LC, and then ligated the BCRs with a polyclonal antibody to Igκ. BCR ligation in cell culture also led to the phosphorylation of BLNK and PLCγ2, which was more pronounced for IgE PCs and IgM PCs compared with IgG1 PCs (Figure 1D), consistent with the relative amounts of surface BCR on these cells.

To determine whether BCR stimulation induced Ca^{2+} flux in IgE PCs, we took advantage of Verigem IgE reporter mice in which IgE-switched cells express the Venus yellow fluorescent protein (Yang et al., 2012). Cultured Verigem B cells were loaded with the Ca^{2+}-sensitive, ratiometric dye Indo-1 and were then stimulated with anti-BCR antibodies. Both IgE PCs and IgE B cells fluxed Ca^{2+}, but IgE PCs exhibited stronger Ca^{2+} flux in response to BCR stimulation with either αIgE or αIgκ (Figure 1E). Together, these findings demonstrate that IgE PCs have elevated mIg which corresponds to increased signaling in response to BCR ligation.

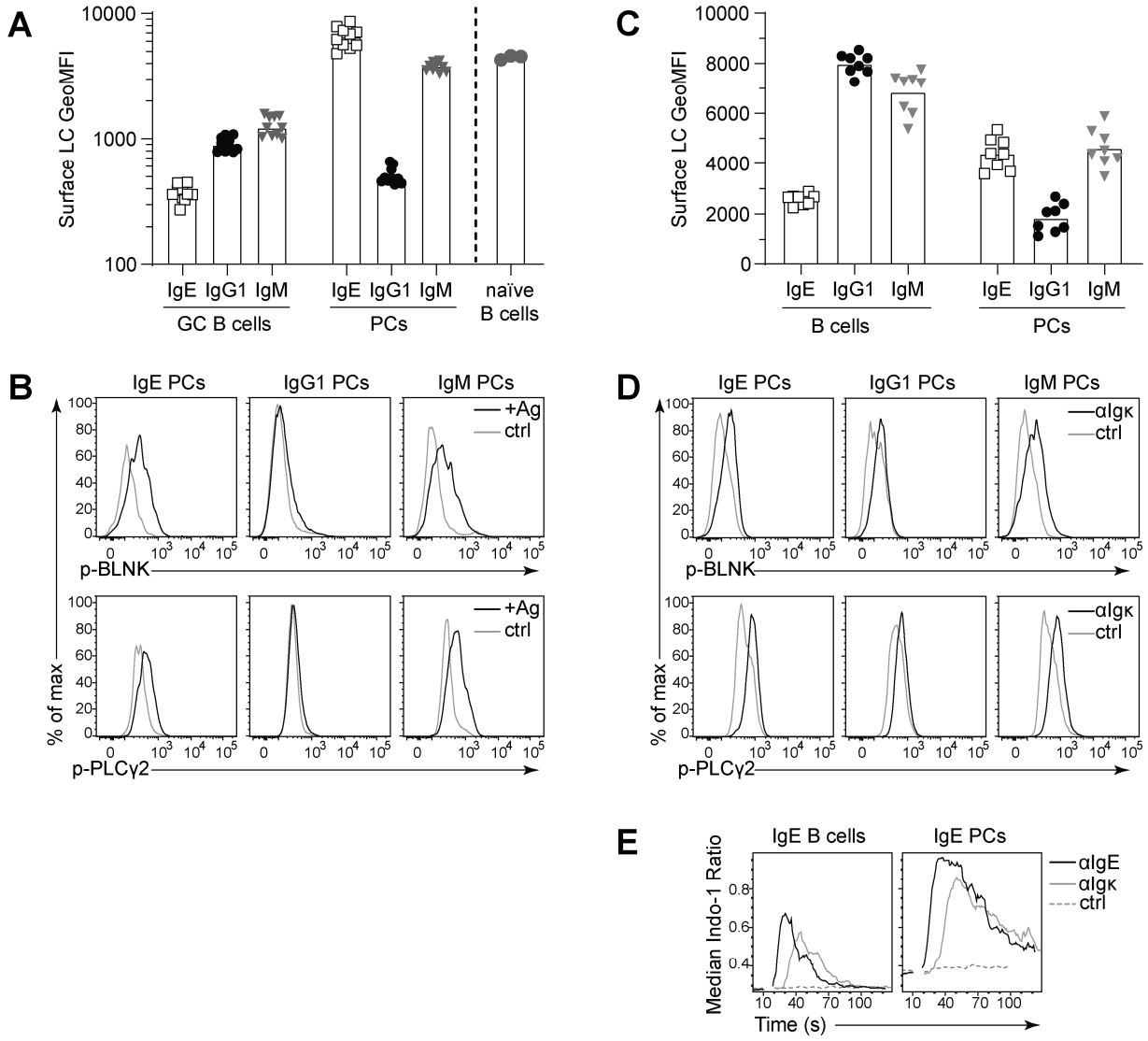

Figure 1. IgE PCs have high surface BCR expression and enhanced signaling in response to antigen. **(A)** Quantification of the surface expression of Igλ LC on the indicated cell types by flow cytometry. B1-8 B cells were adoptively transferred into *Cd19*$^{-/-}$ mice, which were immunized subcutaneously with NP-CGG in alum adjuvant the following day. dLNs were collected 6 days later. After gating on congenic markers to identify transferred B1-8 cells, GC B cells were gated as B220^{hi}CD138^{-}PNA^{+}CD38^{-} and PCs were gated as B220^{int}CD138^{+}. Data for GC B cells and PCs are representative of two independent experiments. For analysis of naïve B cells, splenocytes were isolated from separate B1-8 mice at the time of analysis and cells were gated as B220^{hi}CD38^{+}IgD^{+} Igλ^{+} and NP-binding. **(B)** Phosflow analysis of p-BLNK (upper panels) and p-PLCγ2 (lower panels) after *in vivo* stimulation. Mice were immunized subcutaneously with NP-CGG in alum adjuvant and then, 7 days later, were injected with NP-OVA 15-30 minutes prior to the isolation of dLNs. PCs were gated as B220^{int}CD138^{+}CD38^{lo}IgD^{-}. Data are representative of three independent experiments. **(C)** Quantification of the surface Igλ LC expression on the indicated cell types by flow cytometry. Igλ-enriched B1-8 B cells were cultured for 5.5 days ± 6 hours. Residual

Igκ^{+} B cells were excluded by gating on NP-binding cells. Results are pooled from two independent experiments. B cells were gated as B220^{+}CD138^{-} and PCs were gated as B220^{int}CD138^{+}. **(D)** Phosflow analysis of p-BLNK (upper panels) and p-PLCγ2 (lower panels) after *in vitro* stimulation. Splenocytes from WT mice were cultured for 4 days and then treated with polyclonal goat anti-Igκ F(ab)'2 antibody for 5 min. PCs were gated as B220^{int}IgD^{-}CD138^{+}. Data are representative of four independent experiments. **(E)** Purified Verigem B cells were cultured for 4.5 days, after which cells were stained and loaded with Indo-1. Shown are plots of the median ratio of bound:unbound Indo-1 in IgE B cells (left; identified as Venus^{Lo}CD138^{-}) and IgE PCs (right; identified as Venus^{Hi}CD138^{+}) prior to and following administration of the indicated control or stimulating antibodies. Dots are representative of individual mice (A) or cells from individual mice (D). Bars represent the mean. GeoMFI, geometric mean fluorescence intensity. Please note that the GeoMFI is shown on a log scale in (A) but on a linear scale in (C) for best visualization of the data.

IgE PCs are selectively lost in response to cognate antigen

We next sought to determine the functional consequence of BCR signaling in IgE PCs. In our Igλ-enriched B1-8 B cell culture system, approximately 50-80% of PCs expressed NP-specific BCRs. This allowed us to assess the responsiveness of NP-specific and non-specific IgE PCs in the same culture. When IgE PCs reached peak numbers at day 4.5, we added cognate antigen (NP conjugated to bovine serum albumin, NP-BSA) for BCR stimulation or control antigen (BSA) and then detected NP-specific cells by flow cytometry with total (surface + intracellular) staining with NP-APC. After 24 hours of stimulation, we observed a profound decrease in the proportion of IgE PCs that were NP-binding, whereas there was no change in the proportions of IgG1 or IgM PCs that were NP-binding (Figure 2A). This result indicated that antigen recognition selectively disfavored antigen-specific IgE PCs. In an extensive timecourse analysis, the proportion of IgE PCs that were NP-binding decreased over time to a greater extent than for IgM PCs and IgG1 PCs (Figure 2B). Notably, the proportion of IgM and IgG1 PCs that were NP-specific transiently decreased at intermediate timepoints (6-12h), but by 24 hours had recovered. This phenomenon may have been due to antigen-induced BCR signaling in IgM and IgG1 B cells that promoted the differentiation of new IgM and IgG1 PCs, whereas IgE PC differentiation in cell culture is antigen-independent (Haniuda et al., 2016; Yang et al., 2016). To further assess if the observed reduction in the proportion of NP-binding IgE PCs after NP-BSA treatment was due to a decrease in the number of NP-binding cells or an increase in the number of non-antigen-binding cells, we enumerated these cells over the timecourse. The number of non-antigen specific IgE PCs was constant, whereas the number of NP-specific IgE PCs declined steadily with increasing duration of NP-BSA exposure (Figure 2C). These findings indicate that antigen-mediated stimulation of the BCR on IgE PCs leads to their loss over time.

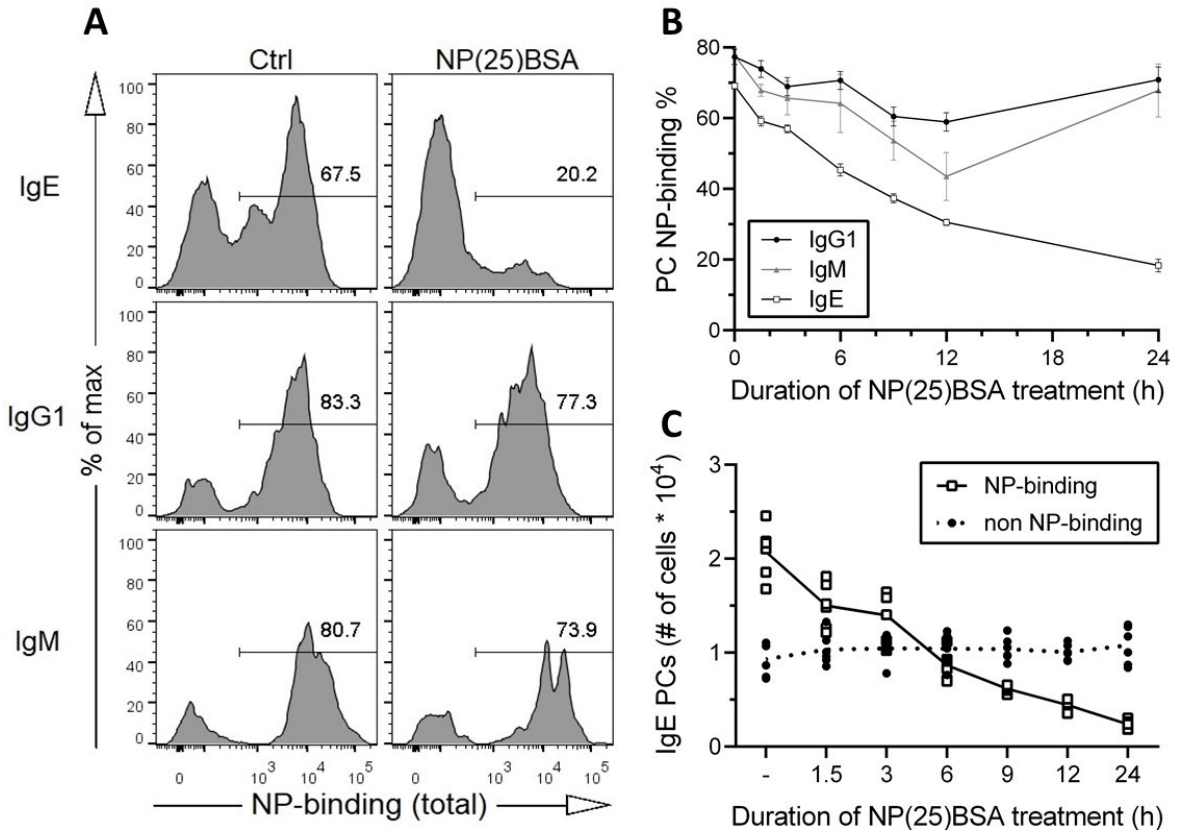

Figure 2. IgE PCs are selectively depleted by cognate antigen over time.

(A-C) Igλ-enriched B1-8 B cells were cultured for 5.5 days ± 6 hours. **(A)** Representative flow cytometry histograms showing the proportion of PCs ($B220^{int}CD138^{+}$) of the indicated isotypes with total (surface + intracellular) binding to NP-APC after 24 ± 3 hours of exposure to either NP(25)BSA (50ng/mL) or control antigen (BSA; 50ng/mL). **(B-C)** NP(25)BSA (50ng/mL) was added at the indicated timepoints, compared with a no antigen control ('0h' in [B] and '-' in [C]), prior to analysis by flow cytometry, as in (A). **(B)** The proportion of PCs of each isotype that bound NP-APC is shown over time. Dots represent the mean of each group (cells from n=6 mice) and error bars reflect standard error. **(C)** The number of IgE PCs that were either NP-binding (white squares) or non-NP binding (black circles) is shown over time. Dots represent cells derived from individual mice (B-C). In (B-C), lines are drawn connecting the mean values. Results are representative of >10 independent experiments (A) or are pooled from two independent experiments (B, C).

The loss of IgE PCs is proportional to the strength of BCR stimulation

We next investigated the relationship between the strength of BCR stimulation and the loss of IgE PCs in our B1-8 B cell culture system. BCR stimulation strength was modulated by altering the dose and valency of NP-BSA treatment for the final 24 hours of the culture and the proportion of IgE PCs that were NP-binding was determined by flow cytometry as above. The depletion of NP-specific IgE PCs was much more pronounced with high-valency NP(25)BSA than with low-valency NP(4)BSA and correlated with the amount of antigen added (Figure 3A). Since IgE PCs express higher surface BCR than IgG1 PCs, we reasoned that IgE PCs would be more sensitive to depletion following BCR stimulation. Therefore, we compared the NP-binding frequency of IgE, IgM, and IgG1 PCs following exposure to NP-BSA of varying doses and valency for 12 hours, a timepoint at which we had previously observed some reductions in PCs of all isotypes. Indeed, while all NP-specific PCs showed valency- and dose-dependent depletion, IgE PCs were depleted to a greater extent than IgG1 PCs, most notably with a high dose of low-valency NP(4)BSA or with a low dose of high-valency NP(25)BSA (Figure 3 Supplement A). As IgM PCs were less abundant under these culture conditions, their responses showed greater variability, but compared with IgE PCs, they were similarly sensitive to low-valency NP(4)BSA, but less sensitive to high-valency NP(25)BSA. Therefore, IgE PCs exhibited enhanced elimination following BCR stimulation compared with IgG1 PCs and in some cases with IgM PCs.

To determine how the affinity and avidity of antigen binding to the BCR affected cognate IgE PC depletion, we took advantage of a B1-8 line with a point mutation that confers 10-fold higher affinity to NP (B1-8hi) (Shih et al., 2002). We co-cultured Igλ-enriched cells from B1-8 and B1-8hi mice and then treated them with low- versus high-valency antigens at different doses as above for 24 hours. Low-valency or low-dose NP-BSA preferentially depleted B1-8hi IgE PCs (Figure 3B and C), indicating that the affinity of IgE PC mIg for antigen is most critical when antigens have low valency or are in low abundance.

As an additional affinity comparison, we took advantage of differences in Igλ LC expression among PCs in the B1-8 culture. A previous study identified two NP-binding populations of B1-8 cells that could be differentiated by their LC expression, one dominated by $Ig\lambda_1$ and the other by $Ig\lambda_2$ (Noviski et al., 2019). We found that PCs derived from Igλ-enriched B1-8 B cells were divisible into three populations with no NP-binding, low NP-binding, and high

NP-binding (Figure 3 supplement B, left). Igλ_1^+ cells were predominantly high NP-binding with a smaller subset that was non-NP-binding, whereas the Igλ_1^- (likely Igλ_2^+) cells were almost entirely intermediate NP-binding (Figure 3 supplement B, right). Among NP-binding PCs (gated as shown in Figure 3 supplement C, left), Igλ_1^+ staining clearly correlated with high NP-binding (Figure 3 supplement C, right), suggesting these cells would have increased sensitivity to cognate antigen. Indeed, low-valency or low-dose NP-BSA preferentially depleted Igλ_1^+ compared with Igλ_1^- IgE PCs (Figure 3D and E), analogous to our results comparing higher-affinity B1-8hi to lower-affinity B1-8 IgE PCs. Taken together, these data provide evidence that the strength of BCR stimulation determines the extent of IgE PC depletion.

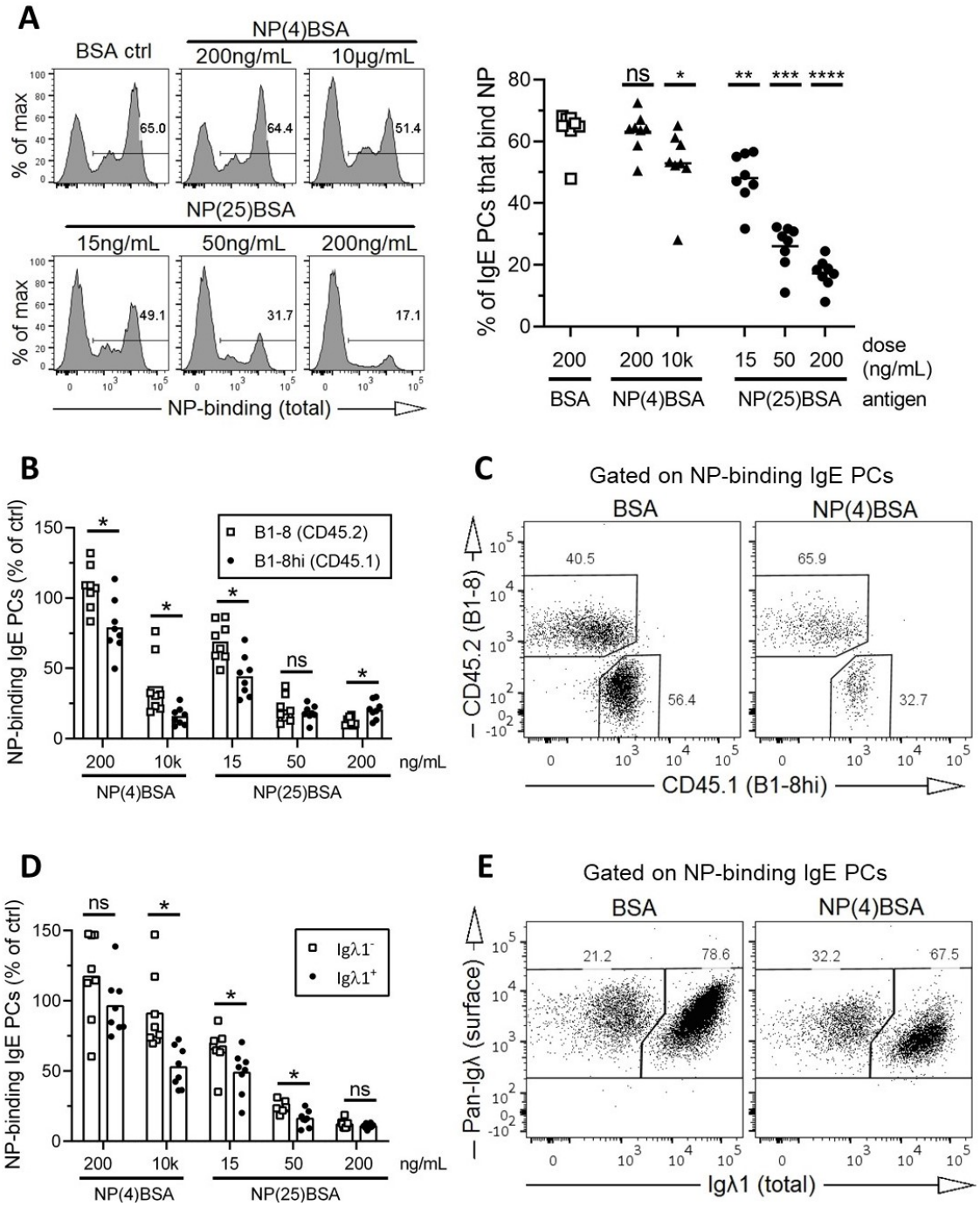

Figure 3. IgE PC depletion by cognate antigen is dose-dependent, affinity-dependent, and avidity-dependent. **(A-E)** Igλ-enriched B cells were cultured for 5.5 days ± 6 hours. The indicated antigens were added to the cultures 24 ± 3 hours prior to analysis by flow cytometry to determine the proportion of IgE PCs that bound to total (surface + intracellular) NP-APC. **(A)** Shown are representative histograms (left) and quantification (right) of the proportion of IgE PCs that were NP-binding after treatment with the indicated antigens. **(B)** Quantification of the number of NP-binding IgE PCs after incubation with the indicated antigens as a percentage of the number of NP-binding IgE PCs in control BSA-treated (200 ng/ml) wells. B cells were derived from B1-8 (white squares) and B1-8hi (black

circles) mice and co-cultured, and then, as in (C), were identified by CD45 congenic markers. **(C)** Representative flow cytometry dot plots showing the proportion of NP-binding IgE PCs that were derived from B1-8 (CD45.2) or B1-8hi (CD45.1) donors after treatment with BSA as a control (200ng/mL) or with NP(4)BSA (10μg/mL). **(D)** Similar to B, except that only B1-8 cells were cultured and NP-binding IgE PCs were categorized as staining negatively (white squares) or positively (black circles) for intracellular $Ig\lambda_1$. **(E)** Representative flow cytometry dot plots showing the proportion of NP-binding IgE PCs that were $Ig\lambda_1^-$ or $Ig\lambda_1^+$ after treatment with BSA or NP(4)BSA, as in (C). IgE PCs were gated as $B220^{int}CD138^+IgE^+$. Dots in (A, B, D) show data points derived from cells from individual mice. n.s., not significant; *, $P < 0.05$; **, $P < 0.01$; ***, $P < 0.001$; ****, $P < 0.0001$ (one-way repeated measures ANOVA with Dunnett's post-test comparing each group to the BSA ctrl [A] or unpaired [B] or paired [D] t tests with the Holm-Sidak correction for multiple comparisons). Bars represent the mean. Data are representative of (A, left panels; C; E) or pooled from (A, right panel; B; D) two independent experiments.

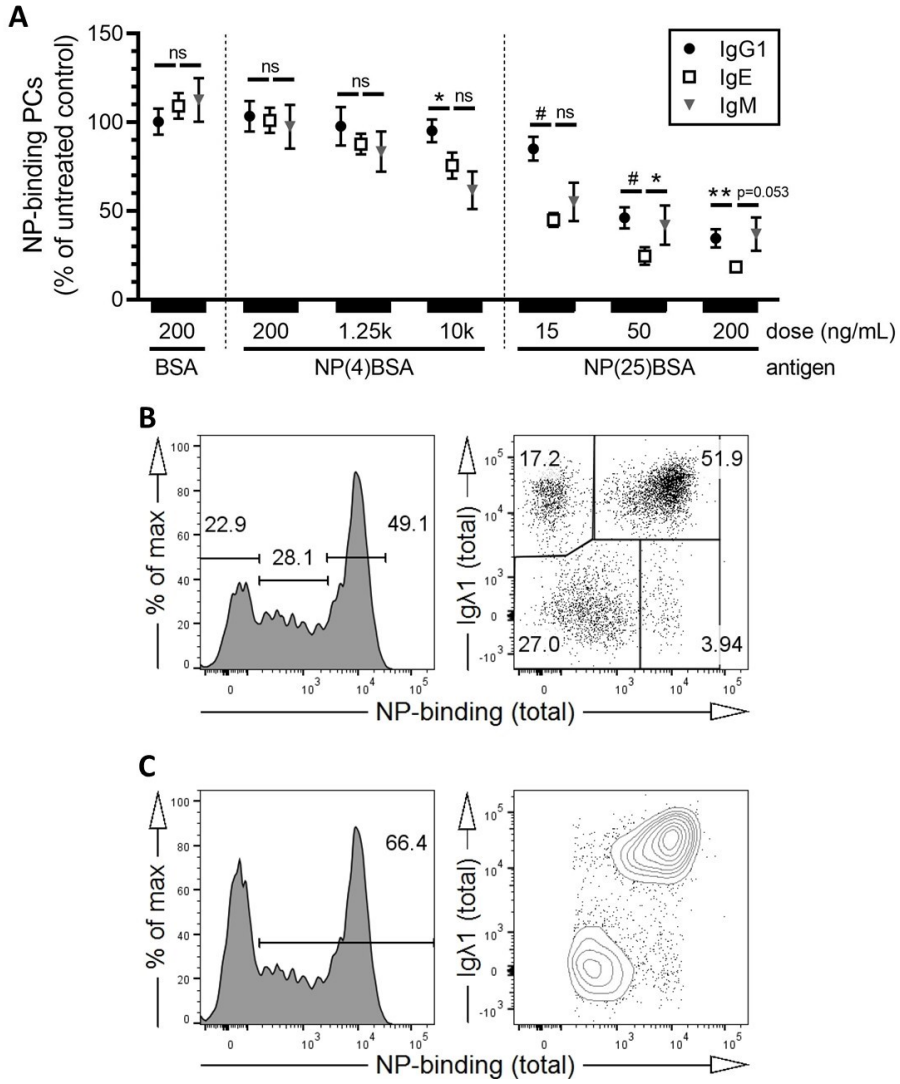

Figure 3 Supplement. (A-C) Igλ-enriched B1-8 B cells were cultured for 5.25 days ± 7 hours and then analyzed by flow cytometry. **(A)** After treatment with the indicated antigens for the final 12 ± 1 hours of the culture, the number of NP-binding PCs of each isotype was quantified by flow cytometry and is shown as a percentage of the number of NP-binding PCs of the same isotype in untreated wells. Dots represent the mean and error bars reflect the standard error, cells from n=14 mice. **(B)** Left, representative flow cytometry histogram of total (surface + intracellular) NP-APC staining of Igλ-expressing IgE PC divided into non-NP-binding, intermediate NP-binding, and high-NP binding gates. Right, representative flow cytometry dot plot of the same cells comparing NP-binding to $Ig\lambda_1$ staining. **(C)** Left, representative flow cytometry histogram of total NP-APC staining of IgE PC divided into NP-binding (intermediate NP-binding + high NP-binding, as depicted in the left panel of B) and non-NP-binding. Right, representative flow cytometry contour plot of IgE PCs gated as NP-binding (as shown in the left panel). (A-C) IgE PCs were gated as $B220^{int}CD138^{+}IgE^{+}$. n.s., not significant; *, $P < 0.05$; **, $P < 0.01$; #, $P < 0.0001$ (two-way ANOVA with Dunnett's post-test comparing IgG1 and IgM to IgE [A]). Data are pooled from (A) or are representative of (B-C) three independent experiments.

IgE PCs undergo apoptosis following BCR stimulation in a cell-intrinsic manner

Our data above were consistent with a model that antigen stimulation of the IgE BCR on IgE PCs resulted in signal transduction leading to apoptosis. However, these data did not exclude the possibility of indirect effects; for example, BCR stimulation could potentially affect the PC differentiation of precursor B cells. To formally establish whether BCR stimulation led to IgE PC apoptosis, we isolated pure populations of IgE PCs, non-IgE PCs, IgE B cells, and non-IgE B cells by sorting live *in vitro*-differentiated Verigem B cells by Venus fluorescence and CD138 staining (Figure 4 Supplement A). Although IgG1- and IgM-expressing cells were indistinguishable at sorting, they were disentangled at the final analysis by staining with anti-isotype antibodies. To determine the effects of BCR stimulation, the sorted cell populations were cultured with αIgκ or control antibody for 24 hours. IgE PCs were depleted 4-fold by BCR stimulation, whereas IgG1 and IgM PCs showed a more modest 2-fold depletion (Figure 4A). This difference was not due to the expression of the Verigem reporter in IgE cells, as in cultures of Verigem-heterozygous cells the Verigem allele did not promote, and in fact was slightly protective against, IgE PC elimination (Figure 4 Supplement B). We hypothesized that IgE PCs were undergoing apoptosis and sought to determine whether BCR stimulation led to an increase in caspase-3 activation. Indeed, we observed a 2-fold increase in active Caspase-3 (aCas3) staining among sorted IgE PCs treated with αIgκ (Figure 4B) but not among IgG1 or IgM PCs. Notably, BCR stimulation improved the survival of sorted IgE, IgG1, and IgM B cells and did not increase caspase-3 activation in these B cells (Figure 4 Supplement C and D). Taken together, these data provide evidence that BCR stimulation of IgE PCs results in caspase-3 activation and apoptosis.

Our studies of sorted PCs showed that apoptotic (aCas3^{+}) PCs of all isotypes lost expression of CD138 (Figure 4C, top). These CD138^{-} aCas3^{+} cells were not contaminating B cells, because they retained similarly high intracellular antibody staining as live PCs (Figure 4C, bottom) and our post-sort purity was routinely 98% or higher (Figure 4 Supplement A, right). Therefore, we identify CD138 downregulation as a general feature of PC apoptosis.

To further characterize PC apoptosis after BCR stimulation without cell sorting, we cultured cells from Blimp1-YFP-transgenic mice, in which YFP expression correlates with Blimp-1 expression and is therefore a marker of PC differentiation. The vast majority of YFP^{+} cells were also marked by CD138, indicating PC identity, but a small proportion of YFP^{+} cells

was CD138$^-$ and stained for aCas3 (Figure 4D), consistent with our prior observations that surface CD138 is lost during PC apoptosis. Treatment with αIgκ, but not control antibody, induced a large (3-4-fold) increase in the proportion of IgE$^+$YFP$^+$ cells that stained for aCas3, whereas only a slight increase in aCas3 staining was observed among IgG1$^+$YFP$^+$ cells and IgM$^+$YFP$^+$ cells (Figure 4D and E). These results were consistent with our findings using sorted cells and provided further evidence that IgE PCs are uniquely sensitive to undergo apoptosis following BCR stimulation.

These observations prompted us to return to our timecourse experiments to examine the kinetics of BCR ligation-induced IgE PC apoptosis. We found that the addition of NP-BSA expanded a population of CD138$^-$IgE^{Hi} cells which was overwhelmingly (>95%) aCas3$^+$ (Figure 4F and Figure 4 Supplement E). This population spiked three hours after BCR stimulation and dwindled slowly thereafter. The proportion of these cells that were NP-binding was increased after NP-BSA treatment compared with control BSA treatment (Figure 4 Supplement E). Therefore, we conclude that these cells are apoptotic antigen-specific IgE PCs. Subsequent to the induction of aCas3, we observed an accumulation of CD138$^-$ IgE^{Hi} IgE PCs that stained with the fixable dye we used to exclude non-viable cells, suggesting these cells had completed apoptosis (Figure 4G). The frequency of NP-binding among these dead cells also increased following NP-BSA treatment (Figure 4 Supplement F). Overall, these findings depict a progression of antigen-specific IgE PCs from live, to apoptotic, to dead following cognate antigen exposure.

Based on previous findings that mice with an anti-apoptotic *Bcl2* transgene expressed in the B cell lineage had markedly increased numbers of IgE PCs (Yang et al., 2012; Yang et al., 2020), we sought to determine whether *Bcl2* overexpression could rescue IgE PCs from depletion after BCR stimulation. IgE PCs derived from *Bcl2*-Tg B1-8 B cells were strongly resistant to cognate antigen-induced elimination, at multiple doses of NP(25)BSA, relative to B1-8 IgE PCs derived from littermates lacking the *Bcl2* transgene (wildtype [WT]; Figure 4H). IgE PCs generated in cultures of polyclonal B cells from *Bcl2*-Tg mice without the B1-8 knock-in were also protected against elimination induced by αBCR antibodies relative to cells from WT littermates, showing no significant depletion even after exposure to αIgE, which depleted more than 75% of WT IgE PCs (Figure 4I and J). These data further support the model that BCR ligation induces apoptosis in IgE PCs, leading to their elimination.

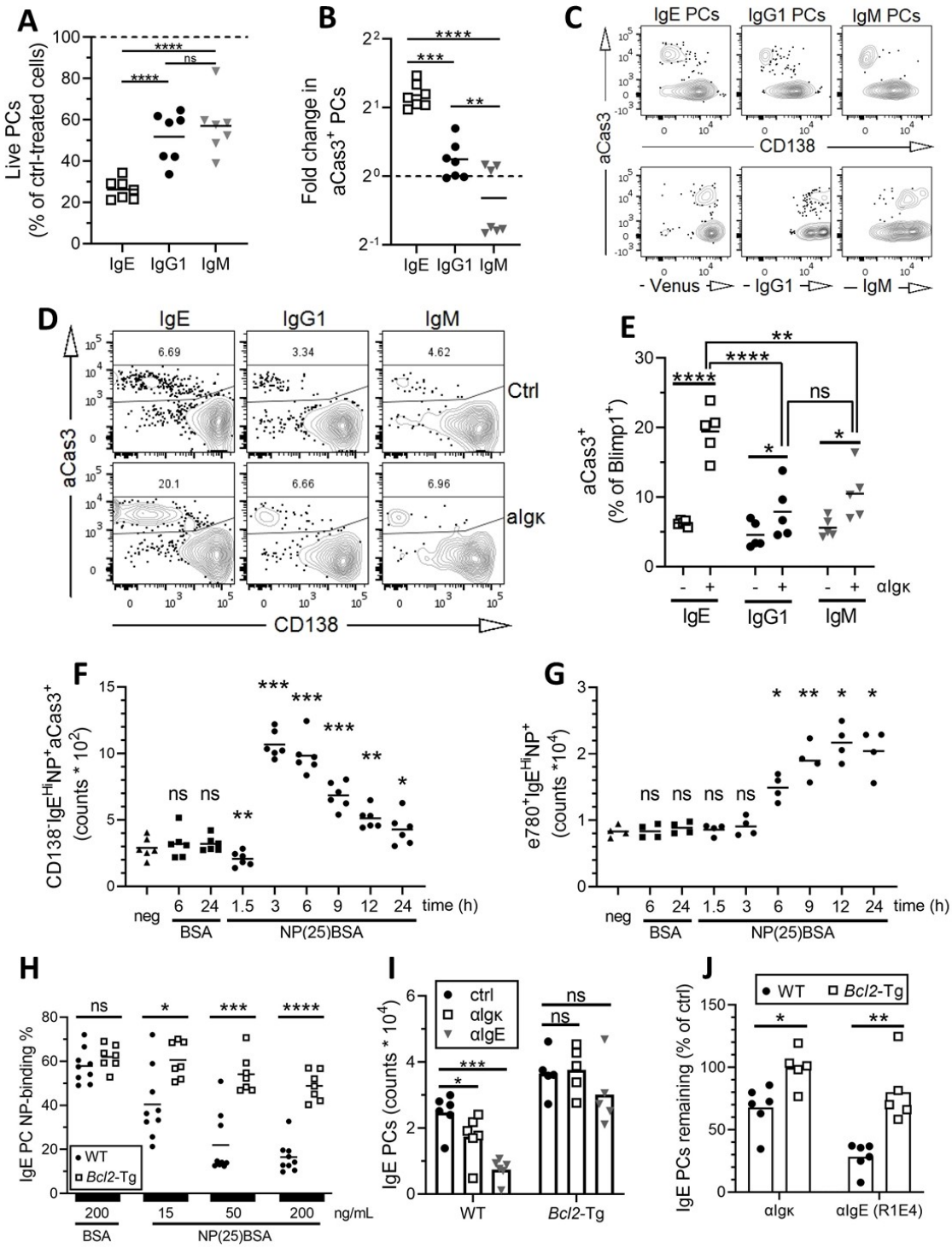

Figure 4. BCR stimulation results in IgE PC apoptosis. (A-C) Purified Verigem B cells were cultured for 4.5 days ± 6 hours, sorted by flow cytometry (see Figure 4 Supplement A), returned to culture, treated with goat polyclonal IgG control or αIgκ antibody for 24 ± 3 hours, and then analyzed by flow cytometry. **(A)** Quantification of the number of live PCs after αIgκ treatment as a percentage of the number of live PCs after control IgG treatment for each isotype. The dotted line represents no change from control. **(B)** Quantification of the fold change in the

proportion aCas3^{+} PCs after αIgκ treatment compared with control IgG treatment for each isotype. The dotted line represents no change from control. **(C)** Representative flow cytometry contour plots of aCas3 versus CD138 staining (top) or aCas3 versus fluorescence/isotype staining (bottom) for the indicated isotypes of PCs treated with αIgκ. **(D-E)** Purified B cells from Blimp1-YFP mice were cultured for 4.5 days and then treated with αIgκ (+) or goat IgG as a control ('ctrl' or '-') for 6 hours prior to analysis by flow cytometry. **(D)** Representative flow cytometry contour plots of aCas3 versus CD138 staining for YFP^{+} cells of the indicated isotypes. **(E)** Quantification of the proportion of YFP^{+} cells of the indicated isotypes that were aCas3^{+}. **(F-G)** Purified B cells from B1-8 mice were cultured for 5.5 days ± 6 hours. Cells were cultured with BSA (control) or NP(25)BSA at the indicated timepoints prior to analysis by flow cytometry, similar to Figure 2B and C. The number of CD138^{-}IgE^{Hi}NP^{+}aCas3^{+} cells **(F)** and e780^{+}IgE^{Hi}NP^{+} cells **(G)** are shown. Cells were gated as shown in Figure 4 Supplement E and F. **(H)** Quantification of the proportion of IgE PCs that were NP-binding after antigen treatment. Igλ-enriched B1-8 B cells from *Bcl2*-Tg (white squares) or control (WT, black circles) littermates were cultured for 5.5 days ± 6 hours and the indicated antigens were added for the final 24 ± 3 hours prior to analysis by flow cytometry. **(I-J)** Polyclonal B cells from *Bcl2*-Tg or WT littermates were purified and cultured for 5.5 days ± 6 hours. At D4.5 ± 6 hours, cells were treated with either αIgκ or αIgE for BCR stimulation, compared with control (goat IgG) treatment. Quantification of the absolute number of IgE PCs **(I)** or the relative percentage of IgE PCs remaining compared to control **(J)** after treatment as indicated. Dots represent data points derived from cells from individual mice. N.s., not significant; *, $P < 0.05$; **, $P < 0.01$; ***, $P < 0.001$; ****, $P < 0.0001$ (one-way ANOVA with Tukey's post-test comparing each group to each other group [A, B], one-way matched ANOVA with the Sidak post-test comparing the indicated pairs of groups [E], one-way matched ANOVA with Dunnett's post test comparing the mean of each group to the negative control [F, G], paired t tests with the Holm-Sidak correction for multiple comparisons [H, J], and two-way ANOVA matched within each genotype with the Sidak post test comparing the mean of each group to the control for each genotype [I]). IgE PCs were gated as B220^{int}CD138^{+}IgE^{+} (H-J). Bars represent the mean. Data are pooled from three (A-B), two (E-G), or four (H-J) independent experiments or are representative of three (C) or two (D) independent experiments.

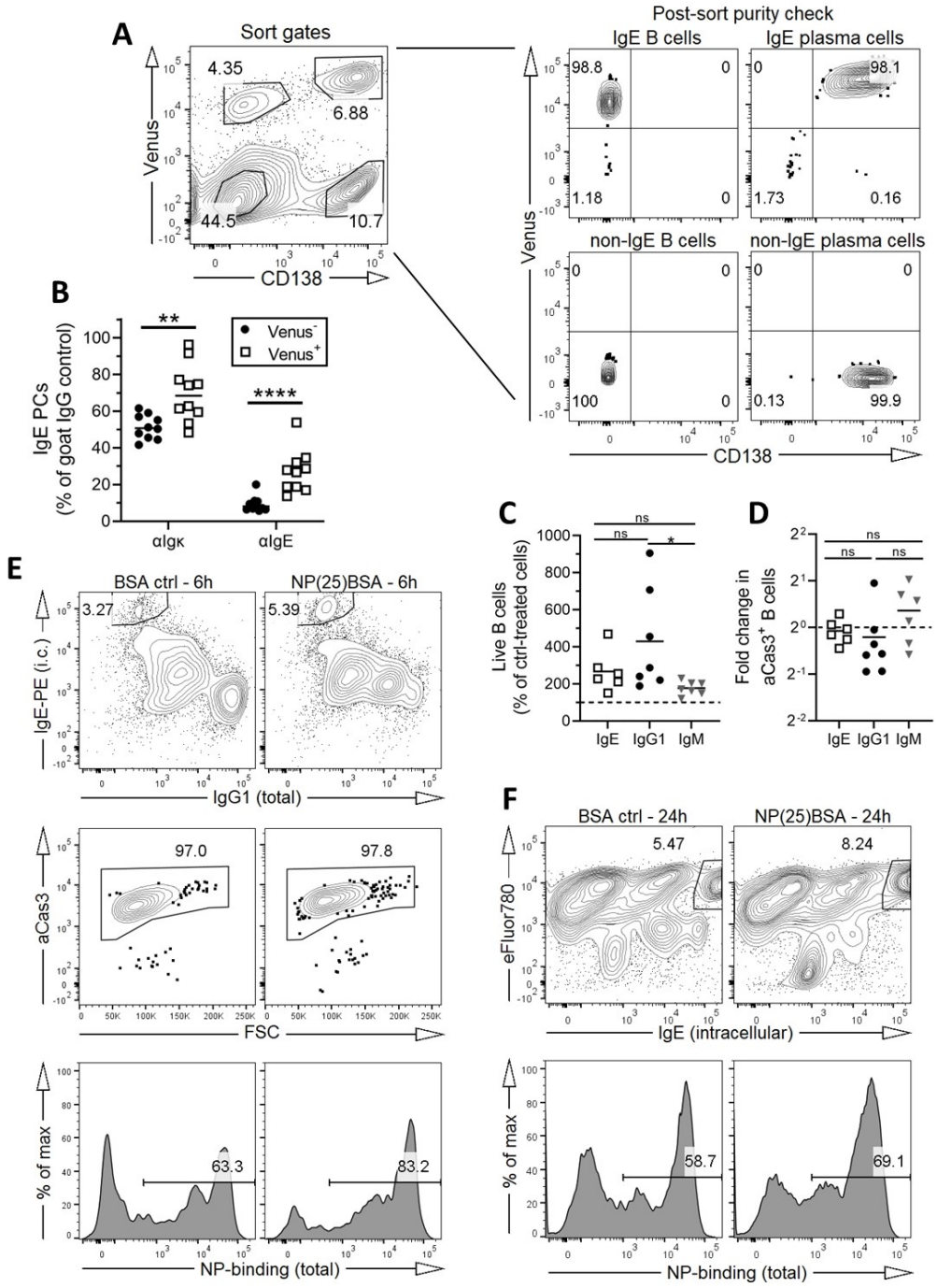

Figure 4 Supplement. **(A)** For the experiments shown in Figure 4A-C, representative flow cytometry contour plots depict the gates used for cell sorting (left) and a confirmation of the purity of sorted cells (right). **(B)** B cells from Verigem heterozygous mice were purified and cultured for 5.5 days ± 6 hours and then analyzed by flow cytometry. 24 ± 3 hours prior to analysis cells were treated with goat IgG control, αIgκ, or αIgE. The relative number of IgE PCs ($B220^{int}CD138^{+}IgE^{+}$) after BCR stimulation is shown as a percentage of the number of IgE PCs after treatment with control IgG with the data segregated by whether the cells expressed the Verigem allele ($Venus^{+}$) or the WT allele ($Venus^{-}$). **(C-D)** Cells were sorted by flow cytometry as shown in (A) and cultured as described in Figure 4A-

C and Methods**.** Sorted cells were cultured separately and treated with either goat polyclonal IgG control or αIgκ antibody for 24 ± 3 hours. **(C)** Quantification of the number of B cells after αIgκ treatment shown as a percentage of the number of B cells after control IgG treatment for each isotype. The dotted line represents no change from ctrl. **(D)** The fold change in the proportion B cells that were $aCas3^{+}$ after αIgκ treatment compared to control IgG treatment. The dotted line represents no change from ctrl. **(E)** Representative flow cytometric analysis of cells from the timecourse analysis in Figure 4F at 6 hours. Cells were gated as $CD138^{-}$ and then sequentially from top to bottom showing the identification of $IgE^{HI}NP^{+}aCas3^{+}$ cells. **(F)** Representative flow cytometric analysis of cells from the timecourse analysis in Figure 4G at 24 hours. Cells were gated sequentially from top to bottom showing the identification of $e780^{+}IgE^{HI}NP^{+}$ cells. Dots represent data points derived from cells from individual mice. n.s., not significant; *, $P < 0.05$; **, $P < 0.01$; ****, $P < 0.0001$ (paired t tests with the Holm-Sidak correction for multiple comparisons [A], one-way unmatched ANOVA with Tukey's post-test comparing each group to each other group [C, D]). Bars represent the mean. Results are representative of three (A) or two (E-F) independent experiments or are pooled from three (B-C) or two (D) independent experiments.

Antigen-induced IgE PC elimination requires the BCR signalosome

In Figure 1, we identified enhanced phosphorylation of BCR signalosome components following mIg stimulation of IgE PCs. Having observed that BCR stimulation led to IgE PC apoptosis, we next determined the contribution of BCR signalosome components to IgE PC elimination. First, we tested the role of Syk, an apical kinase in the BCR signaling phosphorylation cascade, and Btk, a kinase downstream of Syk, with the well-characterized pharmacological inhibitors PRT062607 and ibrutinib, respectively. Inhibition of either kinase dose-dependently rescued IgE PCs from BCR stimulation-induced elimination (Figure 5A and B). However, maximal Syk inhibition achieved a complete rescue, whereas maximal Btk inhibition had a partial effect. BLNK is an adaptor molecule critical for the activation of PLCγ2, which is important for Ca^{2+} flux and other downstream processes, and both BLNK and PLCγ2 were phosphorylated in IgE PCs following BCR stimulation (Figure 1). To test the contribution of these proteins to IgE PC depletion, we targeted the genes encoding these proteins by CRISPR-Cas9 ribonucleoprotein electroporation of B1-8 B cells. Targeting either *Blnk* or *Plcg2* completely blocked antigen-induced IgE PC elimination, whereas electroporation with Cas9 only (without a guide RNA) as a control did not (Figure 5 C and D). We observed similar results with multiple independent guides targeting either *Blnk* or *Plcg2* compared to a non-targeting sgRNA control (Figure 5 supplement A and B). These findings indicate that the mIg ligation-induced elimination of IgE PCs depends upon the activation of the BCR signalosome, with critical contributions from Syk, BLNK, and PLCγ2.

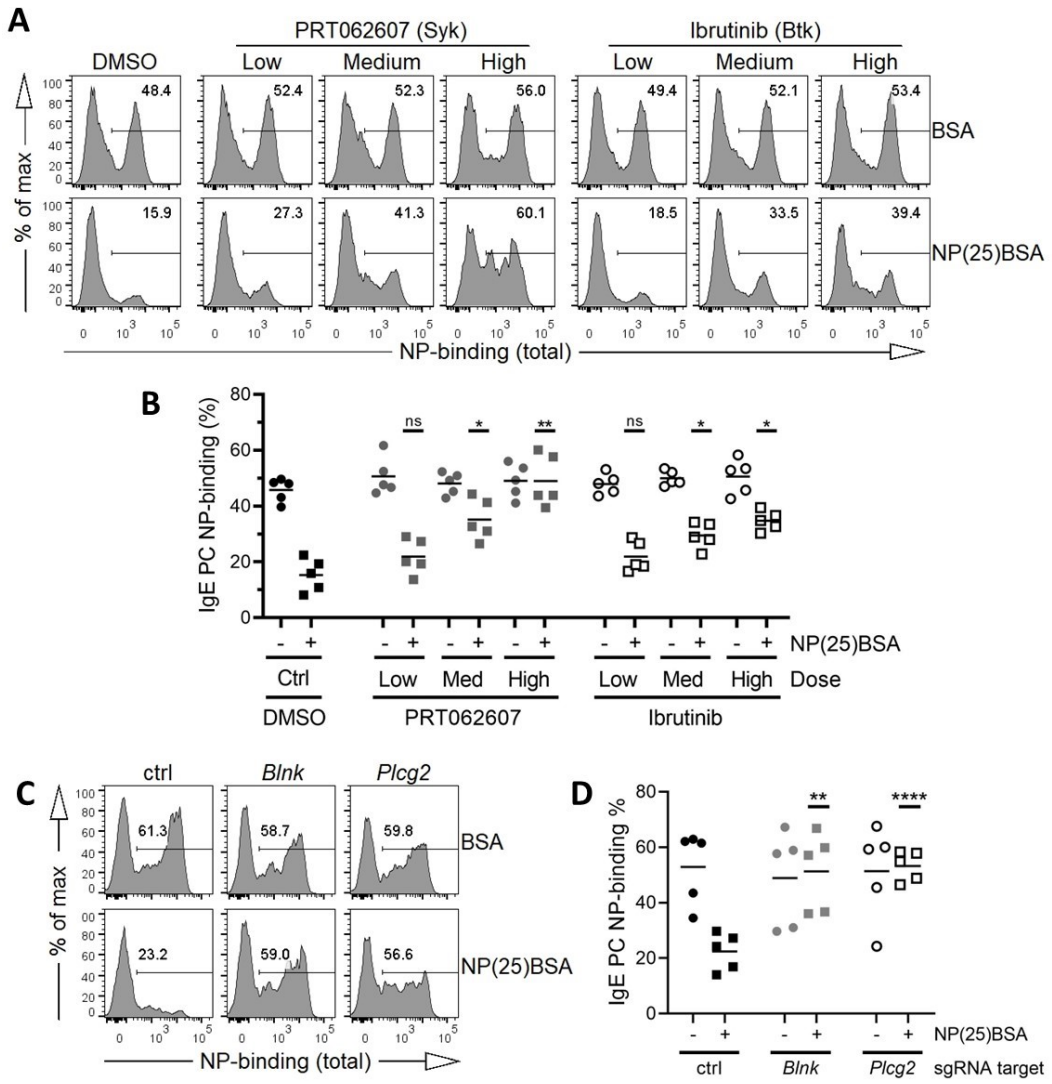

Figure 5. The BCR signalosome is required for mIg ligation-induced IgE PC elimination. (A-B) Igλ-enriched B1-8 B cells were cultured for 4.5 days ± 6 hours and then treated with NP(25)BSA or BSA (50 ng/mL) for 24 ± 3 hours prior to analysis. Shown are representative flow cytometry histograms **(A)** and quantification **(B)** of the proportion of IgE PCs that were NP-binding when cells were treated with the indicated inhibitors or vehicle control (DMSO) prior to incubation with antigen. See Supplementary Table 3 for inhibitor concentrations. **(C-D)** Genes were targeted by electroporation with CRISPR-Cas9 ribonucleoproteins containing the indicated sgRNAs (or no sgRNA as a control) in cultured Igλ-enriched B1-8 B cells (see Methods for details). Representative flow cytometry histograms **(C)** and quantification **(D)** of the proportion of IgE PCs that were NP-binding after treatment with NP(25)BSA or BSA as a control (50-100ng/mL) for 24 ± 3 hours prior to analysis. IgE PCs were gated as $B220^{int}CD138^{+}IgE^{+}$. Dots represent data points derived from cells from individual mice. n.s., not significant; *, $P < 0.05$; **, $P < 0.01$; ****, $P < 0.0001$ (one-way matched ANOVA with Dunnett's post test comparing the mean of each NP(25)BSA-treated inhibitor condition to the NP(25)BSA-treated DMSO control [B] or each NP(25)BSA-treated sgRNA condition to the NP(25)BSA-treated no-sgRNA control [D]). Bars represent the mean. Data are representative of (A, C) or pooled from (B, D) two independent experiments.

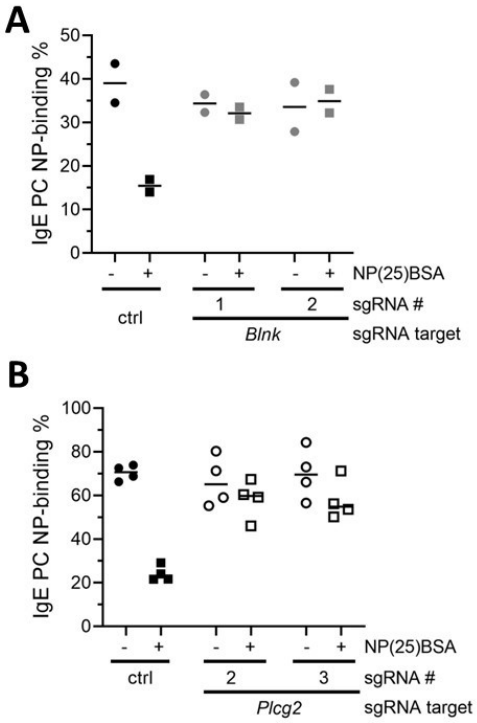

Figure 5 Supplement. (A-B) Genes were targeted by electroporation with CRISPR-Cas9 ribonucleoproteins as described in Figure 5 and Methods. The proportion of IgE PCs that were NP-binding was determined by flow cytometry. Control conditions either received no guide RNA **(A)** or a non-targeting sgRNA **(B)**. IgE PCs were gated as $B220^{int}CD138^{+}IgE^{+}$. Dots represent data points derived from cells from individual mice. Bars represent the mean. Results are representative of two independent experiments.

IgE PCs are constrained by BCR signaling *in vivo*

Having established that activation of the BCR signalosome led to the elimination of IgE PCs *in vitro*, we sought to confirm the importance of BCR signaling in restraining IgE PCs *in vivo*. To this end, we developed a genetic system where BCR signaling could be conditionally impaired exclusively in PCs. Specifically, we bred mice carrying a PC-restricted, tamoxifen-inducible Cre (*Prdm1*$^{\text{tdTomato-Cre/ERT2}}$) (Di Pietro et al., 2022) and a single floxed *Syk* allele (*Syk*$^{\text{flox/+}}$) (Saijo et al., 2003). To ensure Cre activity was restricted to the hematopoietic lineage and to produce matched group sizes sufficient for analysis, we generated bone marrow chimeras using *Prdm1* $^{\text{tdTomato-Cre/ERT2}}$ *Syk*$^{+/+}$ donors as controls. Following immunization and tamoxifen treatment, IgE PCs were selectively increased in frequency (Figure 6A) and abundance (Figure 6 Supplement A) in the dLNs of chimeras derived from *Syk*$^{\text{flox/+}}$ donors compared with chimeras derived from *Syk*$^{+/+}$ donors, whereas other isotypes of PCs and GC B cells were unchanged (Figure 6 Supplement A and B). These findings provide evidence for the selective regulation of IgE PCs *in vivo* by BCR signaling.

To determine whether ligation-induced mIgE signaling would deplete IgE PCs *in vivo*, we took advantage of the unique properties of the R1E4 clone of αIgE that we had previously observed to induce Ca^{2+} flux (Figure 1E) and deplete IgE PCs *in vitro* (Figure 4I and J, Figure 4 Supplement B). WT mice were immunized, and then, after the bulk of IgE PC differentiation had occurred, were administered a single injection of either control antibody, un-modified αIgE R1E4 (Fc-WT), or αIgE R1E4 with a mutated, non-functional Fcγ-receptor binding site (Fc-X). Sixteen hours later, PCs were enumerated in the dLN by flow cytometry. Injection of αIgE R1E4, but not of control antibody, induced a strong decrease in the frequency (Figure 6B and C) and absolute number (Figure 6 Supplement C) of IgE PCs. As expected, PCs of other isotypes were unaffected by αIgE R1E4 injection (Figure 6 Supplement C). The depletion of IgE PCs was equivalent between Fc-WT and Fc-X versions of αIgE R1E4, ruling out a contribution from antibody-dependent cellular cytotoxicity (ADCC) or other BCR-independent mechanisms of IgE PC depletion involving Fcγ receptors. These findings demonstrate that ligation of the BCR on IgE PCs *in vivo* results in IgE PC elimination.

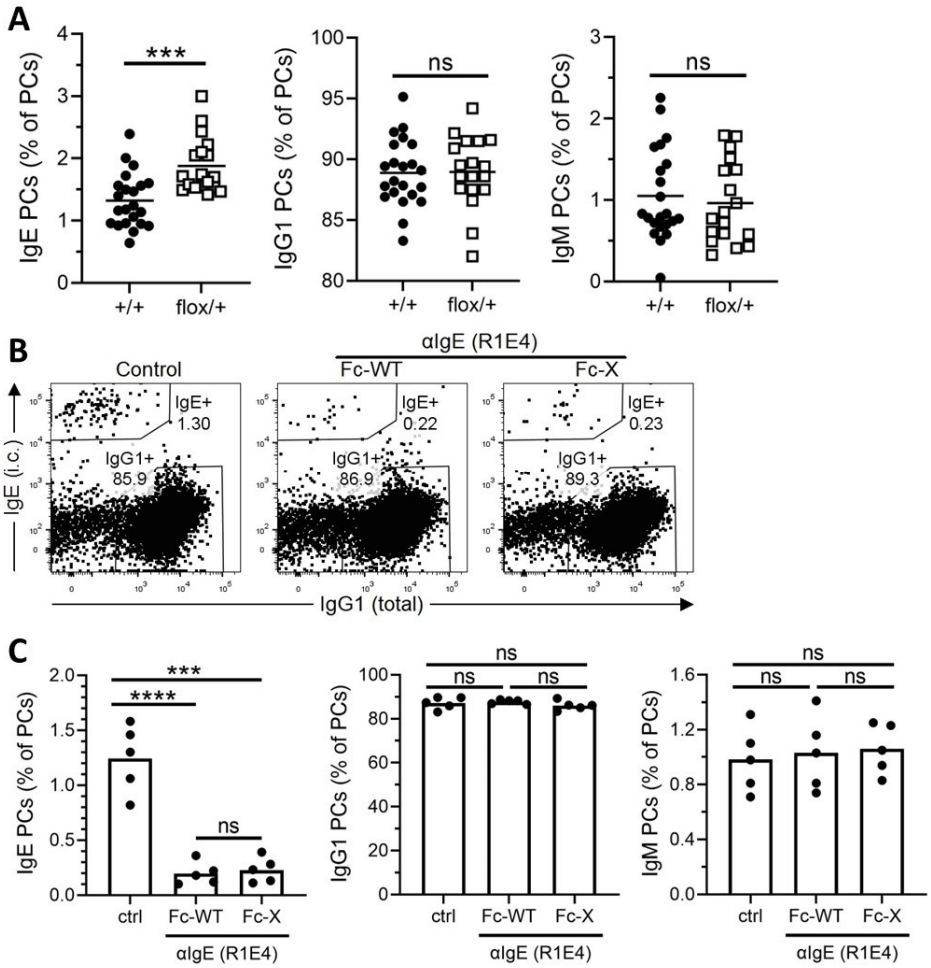

Figure 6. IgE PCs are constrained by BCR signaling *in vivo*. (A) Bone marrow chimeras were generated from *Prdm1*$^{\text{tdTomato-Cre/ERT2}}$ donors that were either *Syk*$^{\text{flox/+}}$ or *Syk*$^{+/+}$ and then immunized with NP-CGG in alum adjuvant after reconstitution. The frequencies of the indicated isotypes of PCs in the dLN were quantified by flow cytometry 9 days after immunization. Tamoxifen was administered to all mice 6, 7, and 8 days after immunization. **(B-C)** WT mice were immunized with NP-CGG in alum adjuvant and then injected intravenously with αIgE R1E4 (with either a normal Fc region [Fc-WT] or with a mutated Fc region [Fc-X]) or control antibody at 7.33 days after immunization. dLNs were analyzed by flow cytometry 16 hours later (8 days after immunization). Representative flow cytometry dot plots **(B)** and quantification **(C)** of the relative frequencies of PCs of the indicated isotypes in the dLN. PCs were gated as CD138^{+}B220^{int}. Dots represent individual mice. n.s., not significant; ***, $P < 0.001$; ****, $P < 0.0001$ (unpaired t tests [A], one-way unmatched ANOVA with Tukey's post-test comparing each group to each other group [C]). Bars represent the mean. Data in (A) are pooled from three experiments and similar results for R1E4 Fc-WT versus ctrl (B-C) were observed in three independent experiments.

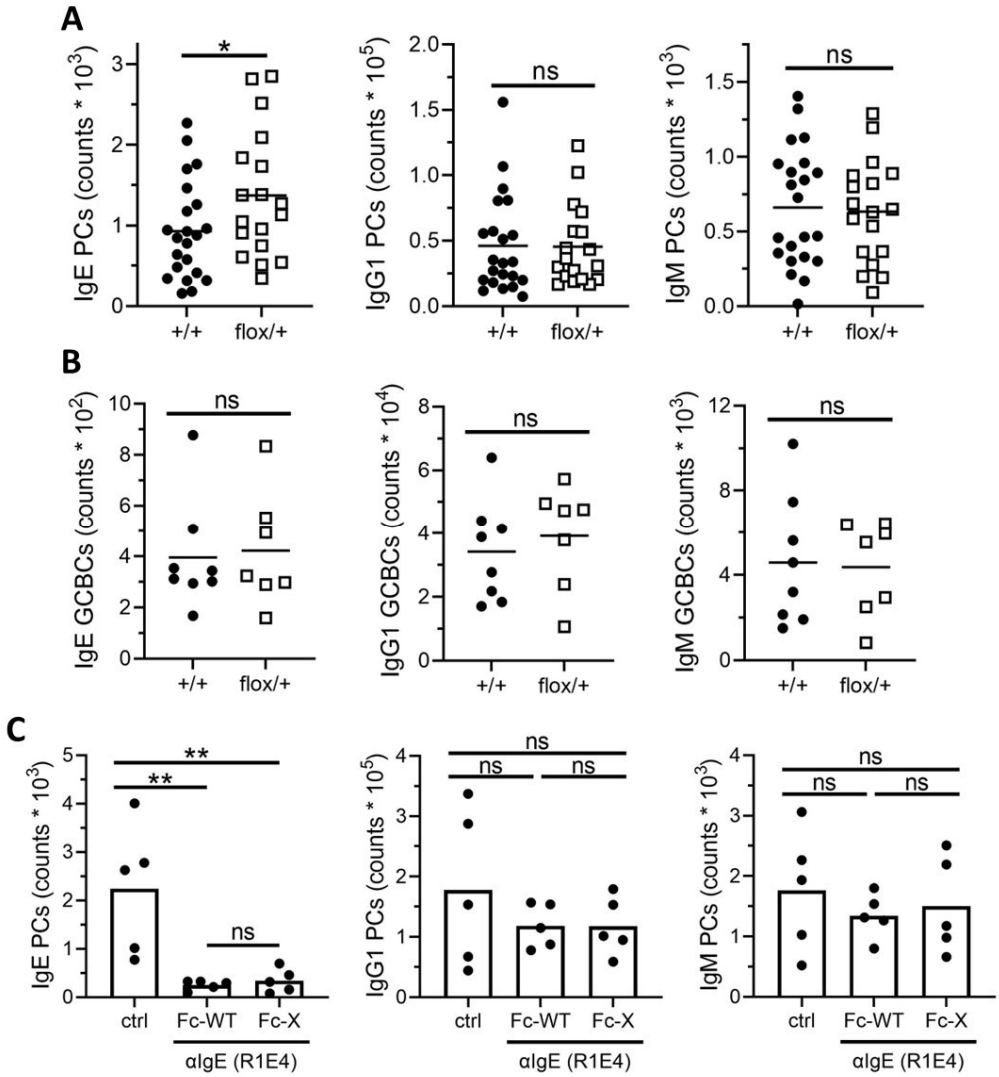

Figure 6 Supplement. (A-B) Bone marrow chimera immunization and tamoxifen treatment was performed as described in Figure 6 and Methods, and cells were enumerated by flow cytometry. Quantification of the number of PCs **(A)** or GC B cells (GCBCs, **[B]**) of the indicated isotypes in the dLN at d9 is shown. **(C)** WT mice were immunized and injected with αIgE or control as described in Figure 6B and C and Methods and analyzed by flow cytometry. Quantification of the number of PCs of the indicated isotypes in the dLN 7 days after immunization is shown. Dots represent individual mice. n.s., not significant; *, $P < 0.05$; **, $P < 0.01$ (unpaired t tests [A-B], one-way unmatched ANOVA with Tukey's post-test comparing each group to each other group [C]). PCs were gated as $B220^{int}CD138^{+}$, GC B cells were gated as $B220^{Hi}CD138^{-}IgD^{-}CD38^{-}$. Bars represent the mean. (A-B) Results are pooled from (A) or representative of (B) three independent experiments and similar results for R1E4 Fc-WT versus ctrl (C) were observed in three independent experiments.

DISCUSSION

Here we reported that IgE PCs had high surface BCR expression that corresponded with the activation of an intracellular signaling cascade in response to antigen exposure. Specifically, BCR stimulation on IgE PCs resulted in the phosphorylation of Syk, BLNK, and PLCγ2 as well as Ca^{2+} flux. This signaling was toxic to IgE PCs, which were depleted proportionally to the strength of BCR stimulation. Consistent with the induction of apoptosis, BCR stimulation resulted in caspase-3 activation in IgE PCs, which could be rescued from cell death by overexpression of a pro-survival *Bcl2* transgene. Through a combination of pharmacological agents and CRISPR gene targeting, we identified Syk, BLNK, and PLCγ2 as key components of the BCR signalosome required for the elimination of IgE PCs after BCR stimulation. In mice, we found that conditional deletion of a single copy of *Syk* in PCs led to a selective increase in the abundance and relative frequency of IgE PCs, indicating that IgE PCs are intrinsically constrained by BCR signaling *in vivo*. Conversely, ligation of mIgE *in vivo* with an αIgE monoclonal antibody led to the elimination of IgE PCs, which we confirmed did not require Fc receptor engagement.

Overall, our data have revealed that IgE PCs are uniquely sensitive to BCR signaling-induced elimination. Quantitative differences in BCR signal transduction may explain the increased sensitivity of IgE PCs to antigen-induced elimination compared with IgG1 PCs. We found that IgE PCs had higher surface mIg expression than IgG1 PCs, which correlated with enhanced phosphorylation of BCR signalosome components after the ligation of mIgE compared with mIgG1. Our studies showing that IgE PC elimination was dependent on the affinity, avidity, and amount of antigen binding to the BCR further reinforce this concept. Our findings also imply that qualitative differences in BCR signaling promote the elimination of IgE PCs relative to IgM PCs. Specifically, we found that IgE and IgM PCs had similar surface mIg expression, yet IgE PCs were more susceptible to apoptosis after BCR stimulation. Furthermore, conditional deletion of *Syk* in PCs *in vivo* led to an increase in IgE PCs but not IgM PCs. The differences in the BCR ligation-induced elimination of IgE and IgM PCs could be related to structural differences between these BCR isotypes. For example, mIgE has an extended cytoplasmic tail (CT), whereas mIgM has a truncated sequence of only three amino acids. The CTs of mIgE and mIgG are thought to prevent recruitment of the inhibitory molecule CD22, which may amplify signaling (Sato et al., 2007). In addition, mIgE and mIgG have a conserved tyrosine motif in

their CTs that is thought to be important for amplification of BCR signal transduction (Engels et al., 2009). The mIgE CT has also been reported to associate with HAX-1, which could play a role in the induction of or protection from apoptosis (Laffleur et al., 2015; Oberndorfer et al., 2006). Arguing against a role for the mIgE CT in promoting IgE PC apoptosis, mice with mutations of the tyrosine motif in the mIgE CT, or truncation of the mIgE CT, have diminished, rather than augmented, IgE responses (Achatz et al., 1997; Schmitt et al., 2020). It is unclear whether this result is due to a role for the mIgE CT in IgE PCs or their activated IgE B cell precursors. Overall, further studies will be needed to elucidate the mechanistic basis for the different functional outcomes of ligation of the IgE BCR versus IgG1 and IgM BCRs in PCs.

BCR ligation may have different functional consequences in PCs compared with B cells. Our cell sorting experiments showed that BCR ligation induced robust caspase-3 activation in IgE PCs, followed by their depletion, with more modest effects on IgG1 and IgM PCs. However, BCR ligation did not induce aCas3 in activated B cells of any isotype (IgE, IgG1 or IgM) and instead actually increased their abundance. These outcomes may be related, in part, to our culture conditions, which included anti-CD40 and IL-4 to mimic T cell help. Previous studies have provided conflicting data on whether there are differences in the survival of IgE versus IgG1 B cells in cell culture without BCR stimulation (Haniuda et al., 2016; Laffleur et al., 2015; Newman and Tolar, 2021; Ramadani et al., 2019; Yang et al., 2016), which we have reviewed in detail (Wade-Vallance and Allen, 2021). These discordant findings could be due to technical differences in culture conditions or analysis methods. Overall, our present data indicate that BCR ligation results in signal transduction that is toxic to IgE PCs, but not to IgE B cells.

The observation that apoptotic PCs lose expression of the marker CD138 also has important implications for the study of apoptosis in the context of IgE responses. Since a large fraction of IgE B cells undergo PC differentiation, apoptotic IgE PCs that have lost CD138 expression could potentially contaminate analyses of IgE B cells. Contamination of dying IgE PCs into IgE B cell flow cytometry gating schemes is especially of concern *in vitro*, where dead cells are not cleared by phagocytes. Therefore, we advise that studies of IgE B cells, especially *in vitro*, should take special precautions to exclude dying IgE PCs, which we found have high intracellular IgE staining. Our results further suggest that future studies of PC apoptosis should utilize markers other than CD138 to identify dying PCs.

The studies presented here involving pharmacological inhibitors and CRISPR-Cas9 targeting revealed that Syk, BLNK, and PLCγ2 were essential for the elimination of IgE PCs after BCR stimulation. In contrast, the inhibition of Btk with ibrutinib only partially rescued IgE PCs. This result was unexpected, given the established role of Btk in activating PLCγ2 downstream of BCR stimulation (Rodriguez et al., 2001; Watanabe et al., 2001). Some residual PLCγ2 phosphorylation was reported in a Btk-deficient B cell line, which may be due to the activity of Syk or Src family kinases (Ozdener et al., 2002; Rodriguez et al., 2001; Takata and Kurosaki, 1996). Alternatively, these findings could be explained by redundancy between Btk and other Tec-family kinases for PLCγ2 activation in IgE PCs. A third possibility is that the requirement for PLCγ2 in BCR stimulation-induced IgE PC elimination involves not only its enzymatic effects but also its reported role in stabilizing the assembly of the BCR signalosome (Wang et al., 2014).

Our findings highlighting a critical role for Syk and BLNK in IgE PC elimination after BCR stimulation provide new insights into prior *in vivo* data. We previously observed that when a single copy of *Syk* was conditionally deleted in activated B cells in mice, this resulted in an increase in the abundance of IgE PCs (Yang et al., 2016). While this could have reflected signaling mediated by Syk in precursor B cells, here we found that conditional deletion of *Syk* in PCs in mice also led to an increase in the abundance of IgE PCs. Together with our cell culture data showing that Syk inhibition prevented IgE PC apoptosis induced by BCR stimulation, our findings suggest that *Syk* heterozygosity directly increases the survival of IgE PCs. In BLNK-deficient mice, IgE PCs accumulated for several weeks, suggesting they were long-lived (Haniuda et al., 2016). While this could have been secondary to enhanced IgE GC B cell responses in these mice, our data here indicate that BLNK-deficiency directly protects IgE PCs from apoptosis after BCR stimulation. Therefore, we propose that the increases in IgE PC responses in mice with perturbations in BCR signal transduction are at least in part due to a direct role for BCR signaling in restraining IgE PC survival.

The idea that BCR signaling in PCs impairs longevity is supported by evidence from mice in which the gene encoding SHP-1, a negative regulator of BCR signaling, was conditionally deleted following B cell activation. These studies identified several features of SHP-1-deficiency that seem reminiscent of IgE responses, including increased PC apoptosis, an abortive GC response, and a reduction in long-lived PCs (Li et al., 2014; Yam-Puc et al., 2021).

One study also identified a role for SHP-1 in PC migration (Li et al., 2014). Interestingly, prior work swapping the mIgE membrane and cytoplasmic domains with those of IgG1 showed that this also affected bone marrow migration (Achatz-Straussberger et al., 2008). However, in the case of SHP-1 this reportedly affected integrin activity (Li et al., 2014) whereas IgE domain swapping reportedly affected migration to CXCL12 (Achatz-Straussberger et al., 2008). Overall, this evidence is consistent with the model that BCR signaling limits IgE PC longevity *in vivo*, and suggests that this could occur through the dual mechanisms of promoting apoptosis and impairing migration to PC survival niches.

The findings reported here, that BCR stimulation induced IgE PC elimination do not exclude a contribution of antigen-independent BCR signaling to the regulation of IgE PC longevity. Elevated BCR expression on IgE PCs may result in increased antigen-independent mIgE signaling relative to IgE B cells, which could negatively impact the survival of IgE PCs. Consistent with this possibility, a recent study reported a higher proportion of IgE PCs than IgG1 PCs had aCas3 staining in an *in vitro* culture system without antigen (Newman and Tolar, 2021). A reduction was noted in the frequency of aCas3^{+} IgE PCs after CRISPR targeting of *Plcg2* or pharmacological inhibition of Syk. However, this latter finding was not compared to IgG1 PCs. Further exploring how antigen-independent and antigen-dependent BCR signaling govern IgE responses represents an important area of future inquiry, especially *in vivo* where immunization with antigen makes it difficult to disentangle antigen-dependent and antigen-independent effects.

While in this study we focused on the antigen-induced elimination of IgE PCs in mice, we also anticipate that these findings will translate to humans. As in mice, human IgE PCs have elevated surface mIgE expression relative to human IgE B cells (Ramadani et al., 2017). Related observations in IgA and IgM PCs are also consistent between mice and humans, including that these cells express elevated mIg and show evidence of BCR signal transduction following mIg ligation (Blanc et al., 2016; Pinto et al., 2013). Similar to our finding that αIgE R1E4 depleted IgE PCs, studies of mice in which a human M1' region was inserted into mIgE showed that treatment with a therapeutic anti-M1' antibody led to a reduction in IgE PCs (Brightbill et al., 2010). While the authors of this study attributed this result to effects of the anti-M1' antibody on IgE B cells that were the precursors of IgE PCs, we propose that this therapy could also directly trigger the apoptosis of IgE PCs. Relatedly, our findings raise the possibility that other human therapeutic anti-IgE monoclonal antibody treatments could ligate mIg on IgE PCs, resulting in

apoptosis. In this regard, we note that the R1E4 clone of αIgE used in our studies only recognizes IgE that is not bound to FcεRI (Keegan et al., 1991), similar to the omalizumab and ligelizumab αIgE therapeutics developed for the treatment of allergic diseases (Gasser et al., 2020). Interestingly, ligelizumab was reported to inhibit IgE production in cell culture (Gasser et al., 2020), which we propose could be due to the elimination of IgE PCs.

Our conclusion that cognate antigen recognition results in IgE PC elimination predicts that the amount of antigen IgE PCs are exposed to may regulate antigen-specific IgE production. Notably, physiological exposures to inhaled aeroallergens in the respiratory tract may be at relatively low doses compared to those used in mouse models of allergic airway disease. Classic studies found that immunization of rodents with low doses of antigen produced more persistent IgE responses (Holt and McMenamin, 1989; Prouvost-Danon et al., 1977; Vaz et al., 1971). Powerful IgE responses can also be provoked by αIgD immunization in mice (Finkelman et al., 1987), which by definition would be unable to ligate mIgE following IgE class switch recombination. Infections with helminth worms are also known to result in dramatic increases in total IgE, yet most of this IgE response is non-specific (Jarrett et al., 1980). In these infections, high doses of antigen exposure could result in the elimination of antigen-specific IgE PCs, favoring the survival of non-antigen-specific IgE PCs. In human food allergy, patients with severe symptoms typically alter their diet to avoid consumption of the foods to which they are allergic. This allergen avoidance may result in enhanced survival of antigen-specific IgE PCs, consistent with the detection of antigen-specific IgE PCs in the blood of patients with peanut allergy (Croote et al., 2018). Conversely, regular oral exposure to food allergens early in life, such as peanut, has been reported to promote allergen-specific tolerance (du Toit et al., 2018). We also note that repeated dosing with increasing amounts of antigen is the key concept underlying allergen immunotherapy. Although such regimens likely have many effects on the immune system, including the induction of antigen-specific IgG4 and impacts on T cells (Akdis and Akdis, 2014), our results suggest they may also limit allergic reactivity through the elimination of antigen-specific IgE PCs. Overall, we propose that the amount of antigen exposure may be an important factor constraining the lifespan of IgE PCs.

Our findings also raise the possibility that genetic variations in molecules involved in BCR signal transduction or apoptosis could affect IgE PC survival. In support of this idea, a wealth of literature links elevated IgE and/or atopy with primary immunodeficiencies or

mutations associated with impairments in antigen receptor signaling pathways (Sokol and Milner, 2018), although these pathways likely also affect B cells and T cells. A recent mutagenesis screen in mice determined that several mutations in genes with a role in BCR signaling, including *Syk* and *Plcg2*, led to increased IgE production (SoRelle et al., 2021). This study estimated that over a third of the human population may be heterozygous carriers for atopy risk alleles that affect BCR signaling or class switch recombination. Even in individuals without inherited alleles that affect BCR signaling or apoptosis, it is possible that sporadic somatic mutations could occur in B cells or PCs that could result in enhanced IgE PC survival in the context of antigen exposure. Our studies have shown that the mutation of even one copy of a gene involved in BCR signal transduction, such as *Syk*, can result in an increase in IgE PC abundance. A potentially important source of somatic mutations in IgE PC precursors could be the GC, in which somatic hypermutation of antibody variable genes occasionally leads to off-target somatic mutations in other regions of the genome, as is well-known from studies of lymphomagenesis (Cyster and Allen, 2019). We therefore propose that inherited and/or somatic mutations that alter BCR signal transduction or apoptosis could result in enhanced survival of antigen-specific IgE PCs in the context of allergy.

The key conclusion of this study is that antigen-driven BCR signaling eliminates IgE PCs, identifying another important way in which the IgE BCR restricts IgE responses. This work establishes a clear functional role for BCR expression on IgE PCs, which has been poorly understood for any PC isotype. It is important to note that our findings do not exclude the possibility of other functional outcomes downstream of BCR activation on IgE PCs or other PC isotypes, such as effects on proliferation, cytoskeletal rearrangements, or metabolism. Human mIgE has multiple splice variants with differences in the extracellular membrane proximal domain, and interestingly these variants have been reported to affect susceptibility of B cell lines to apoptosis after BCR stimulation (Batista et al., 1996; Poggianella et al., 2006). Recent work has further shown a key role for the IgE extracellular membrane proximal domain in surface BCR expression, association with signaling coreceptors, and antigen-independent signaling (Haniuda et al., 2016; Vanshylla et al., 2018; Yang et al., 2016); therefore, it will be important to study how human IgE splice variants affect the functional outcome(s) of BCR signaling in IgE PCs. Overall, we believe that our findings may be of significance for understanding immune tolerance to allergens, with potential therapeutic implications.

MATERIALS AND METHODS

Mice and bone marrow chimeras

All mice used for experiments in this study were on a C57BL/6 (B6) background (backcrossed ≥10 generations). Mice for experiments were sex and age-matched between groups as much as possible and both male and female mice were used. For *in vivo* experimentation, mice were at least 6 weeks of age and for *in vitro* experimentation donor animals were at least 5 weeks of age.

Cd19^{Cre} mice (Rickert et al., 1997), *EμBcl2-22* (*Bcl2*)-Tg mice (Strasser et al., 1991), *Igh-J*^{tm1Dh} mice (Chen et al., 1993), and Verigem mice (Yang et al., 2012) were maintained in our colony on a B6 background. *IgH*$^{B1-8i}$ mice (012642; B6.129P2(C)-*Igh*^{tm2Cgn}/J), *IgH*$^{B1-8hi}$ mice (007594; B6.129P2-*Ptprc*^{a}*Igh*^{tm1Mnz}/J), and *Syk*^{flox} mice (017309; B6.129P2-*Syk*$^{tm1.2Tara}$/J) were purchased from The Jackson Laboratory and then bred in our colony on a B6 background. *Prdm1*$^{tdTomato-Cre/ERT2}$ mice carry an IRES-tdTomato-P2A-CreERT2 construct targeted into the 6th exon of *Prdm1* and will be described in detail elsewhere (Robinson et al., submitted). The following four strains of mice were used as "WT" throughout the manuscript: Boy/J (002014; B6.SJL-*Ptprc*^{a}*Pepc*^{b}/BoyJ), NCI B6-Ly5.1/Cr (originally 01B96; B6-Ly5.2/Cr, later renamed to B6Ly5.1/Cr), B6/J (000664; C57BL/6J), or NCI B6 (556; C57BL/6NCrl). Boy/J and B6/J mice were originally from The Jackson Laboratory and maintained in our colony, while NCI B6-Ly5.1/Cr and NCI B6 were purchased from Charles River.

Mice were housed in specific-pathogen-free facilities. Mouse work was approved by the Institutional Animal Care and Use Committee (IACUC) of the University of California, San Francisco (UCSF). Bone marrow chimeras were generated as described (Yang et al., 2012). We allowed at least 6 weeks for full reconstitution of the chimeras before immunization.

Total B cell purification and Igλ B cell enrichment

All *in vitro* culture experiments were performed with B cells purified by negative selection. B cell purification was generally performed as described (Sullivan et al., 2011) but with the following modifications: Media used was DMEM (Fisher Scientific) containing 4.5 g/L of glucose, 2% fetal bovine serum (FBS, Life Technologies), and 10 mM HEPES (Life Technologies). Centrifugation steps were performed at 400g for 5 minutes. ACK lysis was not

performed. αCD11c biotin (clone N418, Biolegend) was used at 1μL per 10^8 cells, and αTER-119 biotin (clone TER-119, Biolegend) was used at 10μL per 10^8 cells. 100μL of Dynabeads MyOne Streptavidin T1 (Life Technologies) were used per 10^8 cells. In the case of Igλ B cell enrichments, 10μL of αIgκ biotin (clone RMK-12, Biolegend) were added per 10^8 cells and 200μL of Dynabeads MyOne Streptavidin T1 were used per 10^8 cells. After purification, cells were resuspended in complete RPMI (cRPMI), composed of RPMI 1640 without L-glutamine (Fisher Scientific), 10% FBS, 10mM HEPES, 1X Penicillin Streptomycin L-Glutamine (Fisher Scientific), and 50μM β-mercaptoethanol (Fisher Scientific). Final purity was assessed by flow cytometry. Total B cell purity routinely exceeded 98%. For Igλ-enriched purifications ~80% of B cells obtained were routinely $Ig\lambda^+$.

Mouse cell culture and *in vitro* BCR stimulation

All cell culture was performed in a humidified incubator with 5% CO_2 at 37ºC using cRPMI (see above for ingredients) supplemented with 150ng/mL αCD40 (clone FGK-45; Miltenyi Biotec) and 25ng/mL recombinant murine IL-4 (Peprotech) in 96-well Microtest U-bottom plates (BD Falcon) with a volume of 200µl per well. Purified B cells were cultured at a density of 10^4 cells per well, while Igλ-enriched B cells were cultured at 10^3 cells per well. Culture duration varied between experiments as described in figure legends. Cells were plated in triplicate for each condition, except for some timecourse experiments where sextuplicates were used. In some cases, CD45-congenic B cells were co-plated to allow the combined assessment of cells from two different mice, such as in comparisons of B1-8 and B1-8hi B cells. Cell counts from such experiments were scaled up two-fold to account for each sample having had half of the normal cell input.

In vitro BCR stimulation with cognate antigen was performed by adding NP(4)BSA (Biosearch Technologies), NP(25)BSA (Biosearch Technologies), or BSA (Sigma-Aldrich) as a control directly to the culture supernatant without a media swap. See figure legends for timing and doses.

Media swap for *in vitro* experiments with anti-BCR antibodies

In some experiments, a media swap was performed to remove sIg from the culture which would otherwise block anti-BCR antibodies. First, the culture supernatant was removed. Then cells were washed once with pre-warmed cRPMI and resuspended in "swap" cRPMI. This "swap" cRPMI was not freshly prepared, but rather was an aliquot of the initial plating media which was maintained in the incubator throughout the culture period. This strategy ensured that the stimulatory environment of the cells did not change pre- and post-swap, obviating the burst of B cell activation that occurs if fresh stimulatory reagents are used as well as the drop off in viability which occurs if costimulatory signals are completely withdrawn. After the media swap, Goat polyclonal F(ab')2 anti-mouse Igκ (αIgκ; LifeSpan Biosciences), rat anti-mouse IgE clone R1E4, control Chrompure Goat IgG (Jackson ImmunoResearch), or control rat gamma globulin (Jackson ImmunoResearch) was added to achieve a final concentration of 2.5μg/mL.

All inhibitors were diluted in DMSO. The concentration of DMSO in culture never exceeded 0.1% and was typically lower. The specific DMSO vehicle control concentration in each experiment was made to be equivalent to the highest concentration of DMSO in any inhibitor-treated well. Inhibitors were added 5 minutes prior to the addition of stimulating antigen/control. See Supplementary Table 3 for further details on inhibitors and concentrations used.

CRISPR of B1-8 cells

CRISPR gene targeting was achieved by electroporation of ribonucleoprotein complexes containing Cas9 and single guide RNAs (sgRNAs), adapted from a method published for human B cells (Wu et al., 2018). Lyophilized modified sgRNAs (Synthego) were designed using Synthego's sgRNA design tool based on the following criteria in order of importance: 1) cut site within coding region of exon, 2) targeted exon early in coding sequence of protein, 3) cut site early within sequence of exon, 4) high on-target score, 5) target sequence not closely related to off-target sequences. Synthego's negative control sgRNA sequence was used as the negative control sgRNA. sgRNAs were resuspended in TE buffer (Synthego) at 80μM. See Supplementary Table 2 for sgRNA sequences.

Igλ-enriched B1-8 cells were cultured for 2-3 days at 4 $*10^5$ cells/well in a 12-well tissue culture plate (BD Falcon) and then washed, resuspended in cRPMI and counted using a Coulter Counter

Z2 instrument. After all centrifugation steps, 10µL of DNase I was added to the pellet prior to re-suspension. Cells were washed with D-PBS (Fisher Scientific) and then resuspended in 1M buffer (Chicaybam et al., 2013) consisting of RNAse-free H_2O (Life technologies), 5mM KCl (Life technologies), 50mM D-Mannitol (Millipore-Sigma), 15mM $MgCl_2$ (Fisher Scientific), and 120mM $NaH_2PO_4/NaHPO_4$ (Fisher Scientific) at 2.5-10 * 10^6 cells/mL. 18-20µL of cells (4.5-20 *10^4 cells) were then plated into 16-well nucleocuvette strips (Lonza). Each well had also previously received 4µL of ribonucleoprotein, which was pre-assembled by gently mixing 2µL 80µM sgRNA with 2µL 40µM Cas9 (UC Berkeley QB3 MacroLab) and incubating at RT for 15-60 minutes. 1µL of 100µM homology-directed repair template (HDRT) with no homology to the mouse or human genome was added to improve editing efficiency. Cells were then electroporated using an Amaxa 4D nucleofector electroporation with the pulse code EN-138. Following electroporation, "rescue" cRPMI was added to the electroporated wells and cells were incubated for 15 minutes. Afterwards, 7 *10^3 – 3 *10^4 electroporated cells were plated into each well of a previously-prepared culture plate. 2.5-3.5 days following electroporation, cells were stimulated with cognate or control antigen and then analyzed 24 ± 3 hours later by flow cytometry.

<u>Mouse injections (Adoptive transfer, immunization, antibody treatment, and tamoxifen treatment)</u>

Adoptive transfers were performed by intravenous injection of 5 *10^3 Igλ-enriched B1-8 B cells into the retro-orbital plexus of anesthetized mice. Mice were immunized the following day. All immunizations were performed using NP-CGG (Biosearch Technologies) resuspended at 1mg/mL in D-PBS and mixed 50:50 volumetrically with Alhydrogel (Accurate Chemical and Scientific). Mice were injected subcutaneously with 20µL of this solution (10µg of NP-CGG per injection) in each ear. At endpoint, the facial LNs from each side were pooled for analysis (see figure legends for various timepoints).

Unmodified αIgE (clone R1E4; grown from hybridoma), αIgE with a mutated Fc-receptor binding domain (clone R1E4; Cedarlane), or control rat gamma globulin were diluted in D-PBS to a concentration of 0.3mg/mL and injected intravenously to achieve a final dose of 3.25mg/kg. For the experiment shown, mouse gamma globulin was used as a control whereas in previous

experiments that the presented data is representative of rat gamma globulin was used as a control.

Tamoxifen was dissolved at 50mg/mL in corn oil (Sigma-Aldrich) by shaking at 56ºC for several hours. ~100µL/mouse was delivered by intraperitoneal injection to achieve a dose of 200mg/kg.

Production of αIgE clone R1E4

The R1E4 hybridoma was cultured in CELLine bioreactor flasks (Fisher Scientific) in DMEM with Glutamax, 100U/mL Penicillin and 100ug/mL streptomycin, and 55mM β-Mercaptoethanol). The hybridoma was seeded at 10^6 cells/mL in 15 mL 20% FBS in cDMEM, and the nutrient chamber filled with 500-1000 mL 10% FBS in cDMEM. The culture was harvested after seven days and the supernatant purified into PBS by Protein G affinity using a HiTrap Protein G HP affinity column (GE Healthcare), eluted with 0.1M acetic acid (VWR international) pH=3.0 on an AktaPure chromatography system. The eluate was neutralized with $1/10^{th}$ volume of 1.5M NaCl, 1M Tris-HCL pH=8.0 (Fisher Scientific). Fractions containing protein as determined by the A280 absorbance were combined and dialyzed into PBS with 10k MWCO Slide-A-Lyzer dialysis cassettes (Fisher Scientific). The dialysed antibody was concentrated in a 50 MWCO Amicon Ultra Spin column (Fisher Scientific), aliquoted in PBS at 2.5mg/mL, and then frozen at -80ºC until use.

Flow cytometry

For analysis of *in vivo* experiments, cell suspensions were prepared from dLNs as described (Yang et al., 2012), counted using a Coulter Counter Z2 instrument, and then plated in triplicate at a density of $3.5 * 10^6$ cells per staining well. Cells were then stained with antibodies (Supplementary Table 1) essentially as described (Yang et al., 2012). All incubations were 20 minutes on ice except for Fc block incubations (10 minutes) and antibody staining of fixed and permeabilized cells (45 minutes to 1 hour). After the final staining centrifugation step was complete, cells from triplicate staining wells were resuspended and pooled using 100µL FACS buffer (2% FBS and 1mM EDTA [Fisher Scientific] in PBS) and then combined with 7500 AccuCount Ultra Rainbow Fluorescent counting beads (Spherotech; hereafter referred to as counting beads) per sample.

At the endpoint of *in vitro* experiments, supernatants were removed by pipetting, triplicate culture wells (or sextuplicate wells, for some timecourse experiments) were pooled using 100µL FACS buffer per sample, and then the solution of resuspended cells was transferred to a staining plate previously prepared with 7500 counting beads per well. After pelleting and removal of the supernatant, staining was performed as described above for *in vivo* experiments. Cells were then resuspended in 25µL FACS buffer.

For both *in vivo* and *in vitro* experiments, stained cells were then collected on an LSRFortessa (BD). Data were analyzed using FlowJo v10. Counting beads were identified by their high SSC and extreme fluorescence and were used to determine the proportion of the cells plated for staining that had been collected on the flow cytometer for each sample. Cells were gated on FSC-W versus FSC-H and then SSC-W versus SSC-H gates to exclude doublets. Except where otherwise specified, cells were also gated as negative for eFluor780 viability dye and over a broad range of FSC-A to capture resting and blasting lymphocytes. 2D plots were presented as either dot plots or contour plots with outliers shown as dots. In some cases, 'large dots' were used to visualize rare events.

In vivo phosflow experiments

Seven days after immunization, mice were injected with a total of 200µg of NP conjugated to ovalbumin (NP(20)OVA, Biosearch Technologies) in 200µl PBS. Mouse euthanasia was timed so that dLNs could be put in ice-cold PBS 15-30 min after the NP(20)OVA injection. A single cell suspension was prepared on ice, then an equal volume of 4% PFA was added, and immediately transferred to a 37ºC water bath and incubated for 10 minutes. The rest of the protocol was performed as described (Yang et al., 2020), see Supplementary Table 1 for antibodies used.

In vitro phosflow experiments

In vitro phosflow was performed generally as described (Yang et al., 2020). Briefly, cells were incubated with eFluor780 viability dye at RT for 10 min, washed once with PBS, and then resuspended in 100µl cRPMI. Cells were then stimulated with 12.5 µg/ml of goat anti-mouse Igκ

F(ab)'2 and incubated at 37°C for 5 min; then, 100µl of 4% PFA was added, and the sample was incubated at RT for 10 min to stop BCR signaling and fix the cells. The rest of the protocol was performed as described (Yang et al., 2020), see Supplementary Table 1 for antibodies used.

<u>Ca^{2+} flux experiments</u>

All Ca^2 flux experiments were performed with cells from mice compound heterozygous for the Verigem and *Igh-J*^{tm1Dh} IgH alleles. This strategy ensured that mIgE$^+$ BCR expression originated from the Verigem allele, such that all IgE$^+$ cells were Venus$^+$. B cells were purified and cultured as described above for 4.5 days ± 6 hours. Cells were then washed and resuspended in 100µL PBS + 1% FBS. Each time cells were centrifuged, 10µL DNase I (Roche) was added to the pellet prior to re-suspension. Cells were then counted with a Coulter Counter Z2 instrument, diluted to 20 * 10^6 cells/mL, and stained with eFluor780 Fixable Viability Dye (1/1000) and CD138-PE (1/200). Cells were stained for 5-15 minutes at RT or 37ºC. Cells were washed, resuspended in cRPMI at 20 * 10^6 cells/mL, and loaded with the Ca^{2+}-sensitive dye Indo-1 at 0.1µM for 20 minutes at 37ºC. Finally, cells were washed again and resuspended in cRPMI at 20-100 * 10^6 cells/mL and maintained in a water bath at 37ºC prior to flow cytometric analysis. Events were collected on an LSR Fortessa X-20 (BD) for ~10s prior to the addition of anti-BCR antibodies (αIgE clone R1E4 or αIgκ) or control (Goat IgG) at a final concentration of 100µg/mL. After the addition of anti-BCR antibodies, cells were vortexed to mix and returned to the cytometer for observation of Ca^{2+} flux.

<u>Cell sorting experiments</u>

Cell sorting experiments were performed using Verigem-homozygous cells cultured for 4.5 days ± 6 hours. Cells were retrieved from culture, washed, and resuspended in Hank's Balanced Salt Solution (HBSS; obtained from UCSF cell culture facility) supplemented with 1% FBS, 0.5% BSA (Sigma-Aldrich), 2mM EDTA and 10mM HEPES, hereafter known as 'sorting media'. Cells were then counted with a Coulter Counter Z2 instrument, diluted to 20M cells/mL, and stained with 1/1000 e780, 1/200 CD138-PE, and 1/200 IgD-BV510 for 10-30 minutes at RT. Cells were washed, resuspended in HBSS, and diluted to a final concentration of 30 * 10^6 cells/mL in sorting media. Cells were then sorted on a BD FACS Aria II instrument.

Post-sort media was prepared which consisted of 50% FBS 50% cRPMI. Immediately prior to sorting, post-sort media was passed through a 40µm Falcon cell strainer (Fisher Scientific) into a 5mL polypropylene tube (Fisher Scientific). Cells were sorted with a 70µm nozzle at a frequency of 87,000 droplets/second. Immediately following sorting, the purity of sorted populations was verified by flow cytometry. Sorted cells were plated into previously prepared culture plates at 0.5-2 $*10^4$ sorted cells/well. Cells were then treated with anti-BCR antibodies or controls (5µg/mL) as well as with or without various inhibitors and controls and maintained in culture for an additional 24 ± 3 hours prior to flow cytometric analysis.

Statistical analysis

To achieve power to discern meaningful differences, experiments were performed with multiple biological replicates and/or multiple times, see figure legends. The number of samples chosen for each comparison was determined based on past similar experiments to gauge the expected magnitude of differences. GraphPad Prism v9 was used for statistical analyses. Data approximated a log-normal distribution and thus were log transformed for statistical tests. Statistical tests were selected by consulting the GraphPad Statistics Guide according to experimental design. All tests were two-tailed.

SUPPLEMENTARY TABLES

Supplementary Table 1: Antibody-fluorochrome conjugates and other reagents used for flow cytometry

Antibody target or reagent designation	Clone	Company	Conjugate	Dilution
Active Caspase-3	C92-605	BD Biosciences	V450	1/50-100
			FITC	1/25
			Alexa Fluor 647	1/50-100
B220	RA3-6B2	BD Biosciences	V500	1/100-200
		Life Technologies	Qdot 655	1/100-400 (varies by lot)
			APC	1/150-250
CD38	90	Life Technologies	Alexa Fluor 700	1/100
		BD Biosciences	Brilliant Violet 786	1/200
CD45.1	A20	Biolegend	Brilliant Violet 650	1/150-200
		BD Biosciences	Alexa Fluor 647	1/150-200
			Alexa Fluor 700	1/100
CD45.2	104	Biolegend	FITC	1/100-200
			PerCP-Cy5.5	1/100-200
			Brilliant Violet 785	1/100
		BD Biosciences	PerCP-Cy5.5	1/100-200
			PE-Cy7	1/100-200
CD138	281-2	BD Biosciences	PE	1/200
			Brilliant Violet 711	1/150-200
Fixable Viability Dye eFluor 780	N/A	Life Technologies	N/A	1/600-1000
IgD	11-26c.2a	Biolegend	Brilliant Violet 510	1/100-1/200
			Brilliant Violet 711	1/200
			FITC	1/200
			PerCP-Cy5.5	1/200
			Alexa Fluor 700	1/100
IgE	RME1	Biolegend	Unconjugated	1/15
			FITC	1/400-500
			PE	1/350-500
	R35-72	BD Biosciences	Unconjugated	1/15
			Brilliant Violet 650	1/150-300
IgG1	A85-1	BD Biosciences	V450	1/300-400
			FITC	1/300-400
$Ig\lambda_1$	R11-153	BD Biosciences	Biotin	1/300-1/400
$Ig\lambda_{1,2,3}$	R26-46	BD Biosciences	FITC	1/150-200
IgM	II/41	Life Technologies	PE-Cy7	1/175-1/500

NP	N/A	Conjugated in-house as described (Yang et al., 2016).	APC	1/750 of 0.1mg/mL stock
PNA (peanut agglutinin)	N/A	Vector Laboratories	Biotin	1/1000-2000
			FITC	1/500
p-BLNK (pY84)	J117-1278	BD Biosciences	Alexa Fluor 647	1/5
p-PLCγ2 (pY759)	K86-689.37	BD Biosciences	Alexa Fluor 488	1/5
Streptavidin	N/A	Life Technologies	QDot 605	1/400
		BD Biosciences	Brilliant Violet 711	1/400
TruStain FcX (anti-mouse CD16/32)	93	Biolegend	Unconjugated	1/50

Supplementary Table 2: sgRNA sequences

Guide Target and Number (*gene*-#)	**sgRNA sequence**
Negative control	GCACUACCAGAGCUAACUCA
Blnk-1	GAUAUUAAGAACAAUGAAGG
Blnk-2	CCCUUCGAGGAACACUUGGA
Blnk-3	AAGAUAAUCGAUCCAGCCAG
Plcg2-1	GGUGUCCACGUUGACCAUGG
Plcg2-2	GAAGCCUUCAAUCUUGUCUG
Plcg2-3	AGAUAAAGGAAAUCCGUCCG

Supplementary Table 3: Inhibitors

Inhibitor name	**Company**	**Final concentration**		
		"Low"	"Medium"	"High"
Ibrutinib	Gift from Dr. Jack Taunton	500pM	2nM	20nM
PRT062607	Selleck Chemicals	250nM	1μM	4μM

ACKNOWLEDGMENTS

We thank J.B. Jung for assistance with bone marrow chimera experiments; J. Taunton and G.A. Smith for generously providing ibrutinib for our studies; S. Elmes from the Laboratory for Cellular Analysis Core (supported by NIH Grant P30CA082103) for technical assistance with cell sorting experiments; the Gladstone Flow Cytometry Core (supported by NIH Grant P30 AI027763) for their technical support with Ca^{2+} flux experiments; and J.G. Cyster, K.M. Ansel, J. Zikherman, and J.F.E. Koenig for advice and comments on the manuscript.

AUTHOR CONTRIBUTIONS

A.K.W-V., Z.Y., and C.D.C.A. designed the experiments. Z.Y. performed the phosflow experiments and initial apoptosis experiments. J.B.L. performed most inhibitor experiments and assisted with several other experiments. A.K.W-V performed the remainder of the experiments. M.J.R. characterized the *Prdm1*$^{\text{tdTomato-Cre/ERT2}}$ mice and grew the R1E4 hybridoma. D.M.T. supervised the generation of the *Prdm1*$^{\text{tdTomato-Cre/ERT2}}$ mice. C.D.C.A. supervised the research. A.K.W-V. and C.D.C.A. analyzed the data and wrote the paper.

FUNDING

This research was supported by the National Institute of Allergy and Infections Diseases of the National Institutes of Health under Award Number R01AI130470; the Program for Breakthrough Biomedical Research, which is partially funded by the Sandler Foundation; the Sandler Asthma Basic Research Center; and the Cardiovascular Research Institute at the University of California, San Francisco. C.D.C.A. was a Pew Scholar in the Biomedical Sciences, supported by The Pew Charitable Trusts. A.K.W-V was supported by a Doctoral Foreign Study Award from the Canadian Institute of Health Research, funding reference number DFD-170769. D.M.T. and M.J.R. were funded by National Health and Medical Research Council (NHMRC) Australia by an Investigator Award (APP1175411) and Ideas Grant (APP1185294), respectively. The content is solely the responsibility of the authors and does not necessarily represent the official views of the funding agencies.

CONFLICT OF INTEREST STATEMENT

C.D.C.A. is a member of the scientific advisory board for Walking Fish Therapeutics. C.D.C.A.'s spouse is an employee and shareholder of Bristol Myers Squibb. Z.Y. is an employee of Genentech and a shareholder in the Roche Group. These companies had no involvement in this work. The authors have no other financial conflicts of interest to declare.

REFERENCES

Achatz-Straussberger, G., N. Zaborsky, S. Konigsberger, E.O. Luger, M. Lamers, R. Crameri, and G. Achatz. 2008. Migration of antibody secreting cells towards CXCL12 depends on the isotype that forms the BCR. *Eur. J. Immunol.* 38:3167-3177.

Achatz, G., L. Nitschke, and M.C. Lamers. 1997. Effect of transmembrane and cytoplasmic domains of IgE on the IgE response. *Science* 276:409-411.

Akdis, M., and C.A. Akdis. 2014. Mechanisms of allergen-specific immunotherapy: multiple suppressor factors at work in immune tolerance to allergens. *J. Allergy Clin. Immunol.* 133:621-631.

Allen, C.D.C. 2022. Features of B Cell Responses Relevant to Allergic Disease. *J. Immunol.* 208:257-266.

Batista, F.D., S. Anand, G. Presani, D.G. Efremov, and O.R. Burrone. 1996. The two membrane isoforms of human IgE assemble into functionally distinct B cell antigen receptors. *J. Exp. Med.* 184:2197-2205.

Blanc, P., L. Moro-Sibilot, L. Barthly, F. Jagot, S. This, S. de Bernard, L. Buffat, S. Dussurgey, R. Colisson, E. Hobeika, T. Fest, M. Taillardet, O. Thaunat, A. Sicard, P. Mondiere, L. Genestier, S.L. Nutt, and T. Defrance. 2016. Mature IgM-expressing plasma cells sense antigen and develop competence for cytokine production upon antigenic challenge. *Nat. Commun.* 7:13600.

Brightbill, H.D., S. Jeet, Z. Lin, D. Yan, M. Zhou, M. Tan, A. Nguyen, S. Yeh, D. Delarosa, S.R. Leong, T. Wong, Y. Chen, M. Ultsch, E. Luis, S.R. Ramani, J. Jackman, L. Gonzalez, M.S. Dennis, A. Chuntharapai, L. DeForge, Y.G. Meng, M. Xu, C. Eigenbrot, W.P. Lee, C.J. Refino, M. Balazs, and L.C. Wu. 2010. Antibodies specific for a segment of human membrane IgE deplete IgE-producing B cells in humanized mice. *J. Clin. Invest.* 120:2218-2229.

Burgis, S., and A. Gessner. 2007. Unexpected phenotype of STAT6 heterozygous mice implies distinct STAT6 dosage requirements for different IL-4 functions. *Int. Arch. Allergy Immunol.* 143:263-268.

Chen, J., M. Trounstine, F.W. Alt, F. Young, C. Kurahara, J.F. Loring, and D. Huszar. 1993. Immunoglobulin gene rearrangement in B cell deficient mice generated by targeted deletion of the JH locus. *Int. Immunol.* 5:647-656.

Chicaybam, L., A.L. Sodre, B.A. Curzio, and M.H. Bonamino. 2013. An efficient low cost method for gene transfer to T lymphocytes. *PLoS One* 8:e60298.

Croote, D., S. Darmanis, K.C. Nadeau, and S.R. Quake. 2018. High-affinity allergen-specific human antibodies cloned from single IgE B cell transcriptomes. *Science* 362:1306-1309.

Cyster, J.G., and C.D.C. Allen. 2019. B Cell Responses: Cell Interaction Dynamics and Decisions. *Cell* 177:524-540.

Di Pietro, A., J. Polmear, L. Cooper, T. Damelang, T. Hussain, L. Hailes, K. O'Donnell, V. Udupa, T. Mi, S. Preston, A. Shtewe, U. Hershberg, S.J. Turner, N.L. La Gruta, A.W. Chung, D.M. Tarlinton, C.D. Scharer, and K.L. Good-Jacobson. 2022. Targeting BMI-1 in B cells restores effective humoral immune responses and controls chronic viral infection. *Nat. Immunol.* 23:86-98.

du Toit, G., P.H. Sayre, G. Roberts, K. Lawson, M.L. Sever, H.T. Bahnson, H.R. Fisher, M. Feeney, S. Radulovic, M. Basting, M. Plaut, G. Lack, and t. Immune Tolerance Network Learning Early About Peanut Allergy study. 2018. Allergen specificity of early peanut consumption and effect on development of allergic disease in the Learning Early About Peanut Allergy study cohort. *J. Allergy Clin. Immunol.* 141:1343-1353.

Engels, N., L.M. Konig, C. Heemann, J. Lutz, T. Tsubata, S. Griep, V. Schrader, and J. Wienands. 2009. Recruitment of the cytoplasmic adaptor Grb2 to surface IgG and IgE provides antigen receptor-intrinsic costimulation to class-switched B cells. *Nat. Immunol.* 10:1018-1025.

Erazo, A., N. Kutchukhidze, M. Leung, A.P. Christ, J.F. Urban, Jr., M.A. Curotto de Lafaille, and J.J. Lafaille. 2007. Unique maturation program of the IgE response in vivo. *Immunity* 26:191-203.

Finkelman, F.D., C.M. Snapper, J.D. Mountz, and I.M. Katona. 1987. Polyclonal activation of the murine immune system by a goat antibody to mouse IgD. IX. Induction of a polyclonal IgE response. *J. Immunol.* 138:2826-2830.

Gasser, P., S.S. Tarchevskaya, P. Guntern, D. Brigger, R. Ruppli, N. Zbaren, S. Kleinboelting, C. Heusser, T.S. Jardetzky, and A. Eggel. 2020. The mechanistic and functional profile of the therapeutic anti-IgE antibody ligelizumab differs from omalizumab. *Nat. Commun.* 11:165.

Haniuda, K., S. Fukao, T. Kodama, H. Hasegawa, and D. Kitamura. 2016. Autonomous membrane IgE signaling prevents IgE-memory formation. *Nat. Immunol.* 17:1109-1117.

He, J.S., M. Meyer-Hermann, D. Xiangying, L.Y. Zuan, L.A. Jones, L. Ramakrishna, V.C. de Vries, J. Dolpady, H. Aina, S. Joseph, S. Narayanan, S. Subramaniam, M. Puthia, G. Wong, H. Xiong, M. Poidinger, J.F. Urban, J.J. Lafaille, and M.A. Curotto de Lafaille. 2013. The distinctive germinal center phase of IgE+ B lymphocytes limits their contribution to the classical memory response. *J. Exp. Med.* 210:2755-2771.

Holt, P.G., and C. McMenamin. 1989. Defence against allergic sensitization in the healthy lung: the role of inhalation tolerance. *Clin. Exp. Allergy* 19:255-262.

Jarrett, E., S. Mackenzie, and H. Bennich. 1980. Parasite-induced `nonspecific' IgE does not protect against allergic reactions. *Nature* 283:302-303.

Jimenez-Saiz, R., Y. Ellenbogen, K. Bruton, P. Spill, D.D. Sommer, H. Lima, S. Waserman, S.U. Patil, W.G. Shreffler, and M. Jordana. 2019. Human BCR analysis of single-sorted,

putative IgE(+) memory B cells in food allergy. *J. Allergy Clin. Immunol.* 144:336-339 e336.

Keegan, A.D., C. Fratazzi, B. Shopes, B. Baird, and D.H. Conrad. 1991. Characterization of New Rat Anti-Mouse Ige Monoclonals and Their Use Along with Chimeric Ige to Further Define the Site That Interacts with Fc-Epsilon-Rii and Fc-Epsilon-Ri. *Mol. Immunol.* 28:1149-1154.

Laffleur, B., S. Duchez, K. Tarte, N. Denis-Lagache, S. Peron, C. Carrion, Y. Denizot, and M. Cogne. 2015. Self-Restrained B Cells Arise following Membrane IgE Expression. *Cell Rep.* 10:900-909.

Li, Y.F., S. Xu, X. Ou, and K.P. Lam. 2014. Shp1 signalling is required to establish the long-lived bone marrow plasma cell pool. *Nat. Commun.* 5:4273.

Muller, U., W. Stenzel, G. Kohler, T. Polte, M. Blessing, A. Mann, D. Piehler, F. Brombacher, and G. Alber. 2008. A gene-dosage effect for interleukin-4 receptor alpha-chain expression has an impact on Th2-mediated allergic inflammation during bronchopulmonary mycosis. *J. Infect. Dis.* 198:1714-1721.

Newman, R., and P. Tolar. 2021. Chronic calcium signaling in IgE(+) B cells limits plasma cell differentiation and survival. *Immunity* 54:2756-2771 e2710.

Noviski, M., C. Tan, J. Huizar, V. Vykunta, J.L. Mueller, and J. Zikherman. 2019. Optimal Development of Mature B Cells Requires Recognition of Endogenous Antigens. *J. Immunol.* 203:418-428.

Oberndorfer, I., D. Schmid, R. Geisberger, G. Achatz-Straussberger, R. Crameri, M. Lamers, and G. Achatz. 2006. HS1-associated protein X-1 interacts with membrane-bound IgE: impact on receptor-mediated internalization. *J. Immunol.* 177:1139-1145.

Ozdener, F., C. Dangelmaier, B. Ashby, S.P. Kunapuli, and J.L. Daniel. 2002. Activation of phospholipase Cgamma2 by tyrosine phosphorylation. *Mol. Pharmacol.* 62:672-679.

Pinto, D., E. Montani, M. Bolli, G. Garavaglia, F. Sallusto, A. Lanzavecchia, and D. Jarrossay. 2013. A functional BCR in human IgA and IgM plasma cells. *Blood* 121:4110-4114.

Poggianella, M., M. Bestagno, and O.R. Burrone. 2006. The extracellular membrane-proximal domain of human membrane IgE controls apoptotic signaling of the B cell receptor in the mature B cell line A20. *J. Immunol.* 177:3597-3605.

Prouvost-Danon, A., D. Mouton, A. Abadie, J.C. Mevel, and G. Biozzi. 1977. Genetic regulation of IgE and agglutinating antibody synthesis in lines of mice selected for high and low immune responsiveness. *Eur. J. Immunol.* 7:342-348.

Ramadani, F., H. Bowen, H.J. Gould, and D.J. Fear. 2019. Transcriptional Analysis of the Human IgE-Expressing Plasma Cell Differentiation Pathway. *Front. Immunol.* 10:402.

Ramadani, F., H. Bowen, N. Upton, P.S. Hobson, Y.C. Chan, J.B. Chen, T.W. Chang, J.M. McDonnell, B.J. Sutton, D.J. Fear, and H.J. Gould. 2017. Ontogeny of human IgE-expressing B cells and plasma cells. *Allergy* 72:66-76.

Rickert, R.C., J. Roes, and K. Rajewsky. 1997. B lymphocyte-specific, Cre-mediated mutagenesis in mice. *Nucleic Acids Res.* 25:1317-1318.

Robinson, M.J., M. Prout, H. Mearns, R. Kyle, M. Camberis, E.E. Forbes-Blom, W.E. Paul, C.D. Allen, and G. Le Gros. 2017. IL-4 Haploinsufficiency Specifically Impairs IgE Responses against Allergens in Mice. *J. Immunol.* 198:1815-1822.

Rodriguez, R., M. Matsuda, O. Perisic, J. Bravo, A. Paul, N.P. Jones, Y. Light, K. Swann, R.L. Williams, and M. Katan. 2001. Tyrosine residues in phospholipase Cgamma 2 essential for the enzyme function in B-cell signaling. *J. Biol. Chem.* 276:47982-47992.

Saijo, K., C. Schmedt, I.H. Su, H. Karasuyama, C.A. Lowell, M. Reth, T. Adachi, A. Patke, A. Santana, and A. Tarakhovsky. 2003. Essential role of Src-family protein tyrosine kinases in NF-kappaB activation during B cell development. *Nat. Immunol.* 4:274-279.

Sato, M., T. Adachi, and T. Tsubata. 2007. Augmentation of Signaling through BCR Containing IgE but not That Containing IgA Due to Lack of CD22-Mediated Signal Regulation. *J. Immunol.* 178:2901-2907.

Schmitt, M.E.R., J. Lutz, P. Haase, M.R. Bosl, J. Wienands, N. Engels, and D. Voehringer. 2020. The B-cell antigen receptor of IgE-switched plasma cells regulates memory IgE responses. *J. Allergy Clin. Immunol.* 146:642-651 e645.

Shih, T.A., E. Meffre, M. Roederer, and M.C. Nussenzweig. 2002. Role of BCR affinity in T cell dependent antibody responses in vivo. *Nat. Immunol.* 3:570-575.

Sokol, K., and J.D. Milner. 2018. The overlap between allergy and immunodeficiency. *Curr. Opin. Pediatr.* 30:848-854.

Sonoda, E., Y. Pewzner-Jung, S. Schwers, S. Taki, S. Jung, D. Eilat, and K. Rajewsky. 1997. B cell development under the condition of allelic inclusion. *Immunity* 6:225-233.

SoRelle, J.A., Z. Chen, J. Wang, T. Yue, J.H. Choi, K.W. Wang, X. Zhong, S. Hildebrand, J. Russell, L. Scott, D. Xu, X. Zhan, C.H. Bu, T. Wang, M. Choi, M. Tang, S. Ludwig, X. Zhan, X. Li, E.M.Y. Moresco, and B. Beutler. 2021. Dominant atopy risk mutations identified by mouse forward genetic analysis. *Allergy* 76:1095-1108.

Strasser, A., S. Whittingham, D.L. Vaux, M.L. Bath, J.M. Adams, S. Cory, and A.W. Harris. 1991. Enforced BCL2 expression in B-lymphoid cells prolongs antibody responses and elicits autoimmune disease. *Proc. Natl. Acad. Sci. U. S. A.* 88:8661-8665.

Sullivan, B.M., H.E. Liang, J.K. Bando, D. Wu, L.E. Cheng, J.K. McKerrow, C.D. Allen, and R.M. Locksley. 2011. Genetic analysis of basophil function in vivo. *Nat. Immunol.* 12:527-535.

Takata, M., and T. Kurosaki. 1996. A role for Bruton's tyrosine kinase in B cell antigen receptor-mediated activation of phospholipase C-gamma 2. *J. Exp. Med.* 184:31-40.

Vanshylla, K., F. Opazo, K. Gronke, J. Wienands, and N. Engels. 2018. The extracellular membrane-proximal domain of membrane-bound IgE restricts B cell activation by limiting B cell antigen receptor surface expression. *Eur. J. Immunol.* 48:441-453.

Vaz, E.M., N.M. Vaz, and B.B. Levine. 1971. Persistent formation of reagins in mice injected with low doses of ovalbuminl. *Immunology* 21:11-15.

Wade-Vallance, A.K., and C.D.C. Allen. 2021. Intrinsic and extrinsic regulation of IgE B cell responses. *Curr. Opin. Immunol.* 72:221-229.

Wang, J., H. Sohn, G. Sun, J.D. Milner, and S.K. Pierce. 2014. The autoinhibitory C-terminal SH2 domain of phospholipase C-gamma2 stabilizes B cell receptor signalosome assembly. *Sci Signal* 7:ra89.

Watanabe, D., S. Hashimoto, M. Ishiai, M. Matsushita, Y. Baba, T. Kishimoto, T. Kurosaki, and S. Tsukada. 2001. Four tyrosine residues in phospholipase C-gamma 2, identified as Btk-dependent phosphorylation sites, are required for B cell antigen receptor-coupled calcium signaling. *J. Biol. Chem.* 276:38595-38601.

Wu, C.M., T.L. Roth, Y. Baglaenko, D.M. Ferri, P. Brauer, J.C. Zuniga-Pflucker, K.W. Rosbe, J.E. Wither, A. Marson, and C.D.C. Allen. 2018. Genetic engineering in primary human B cells with CRISPR-Cas9 ribonucleoproteins. *J. Immunol. Methods* 457:33-40.

Yam-Puc, J.C., L. Zhang, R.A. Maqueda-Alfaro, L. Garcia-Ibanez, Y. Zhang, J. Davies, Y.A. Senis, M. Snaith, and K.M. Toellner. 2021. Enhanced BCR signaling inflicts early plasmablast and germinal center B cell death. *iScience* 24:102038.

Yang, Z., M.J. Robinson, X. Chen, G.A. Smith, J. Taunton, W. Liu, and C.D. Allen. 2016. Regulation of B cell fate by chronic activity of the IgE B cell receptor. *Elife* 5:e21238.

Yang, Z., B.M. Sullivan, and C.D. Allen. 2012. Fluorescent in vivo detection reveals that IgE(+) B cells are restrained by an intrinsic cell fate predisposition. *Immunity* 36:857-872.

Yang, Z., C.M. Wu, S. Targ, and C.D.C. Allen. 2020. IL-21 is a broad negative regulator of IgE class switch recombination in mouse and human B cells. *J. Exp. Med.* 217:e20190472.